Taylor & Francis
Taylor & Francis Group

Particulate Science and Technology

An International Journal

ISSN: (Print) (Online) Journal homepage: https://www.tandfonline.com/loi/upst20

Functionality improvement of Chlorzoxazone by crystallo-co-agglomeration using multivariate analysis approach

Mihir K. Raval , Kevin C. Garala , Jaydeep M. Patel , Rajesh K. Parikh & Navin R. Sheth

To cite this article: Mihir K. Raval , Kevin C. Garala , Jaydeep M. Patel , Rajesh K. Parikh & Navin R. Sheth (2020): Functionality improvement of Chlorzoxazone by crystallo-co-agglomeration using multivariate analysis approach, Particulate Science and Technology, DOI: 10.1080/02726351.2020.1799126

To link to this article: https://doi.org/10.1080/02726351.2020.1799126

Published online: 30 Jul 2020.

PARTICULATE SCIENCE AND TECHNOLOGY
https://doi.org/10.1080/02726351.2020.1799126

Taylor & Francis
Taylor & Francis Group

Functionality improvement of Chlorzoxazone by crystallo-co-agglomeration using multivariate analysis approach

Mihir K. Raval[a], Kevin C. Garala[b], Jaydeep M. Patel[a], Rajesh K. Parikh[c], and Navin R. Sheth[d]

[a]Department of Pharmaceutical Sciences, Saurashtra University, Rajkot, Gujarat, India; [b]Atmiya Institute of Pharmacy, Rajkot, Gujarat, India; [c]L. M. College of Pharmacy, Ahmedabad, Gujarat, India; [d]Gujarat Technological University, Ahmedabad, Gujarat, India

ABSTRACT

The aim of present work was to improve physicochemical properties of model drug Chlorzoxazone by crystallo-co-agglomeration (CCA) in the presence of different polymers and excipients. Identification of Quality Target Product Profile and Critical Quality Attributes were done using Risk assessment and Failure mode effect analysis. CCA was formulated by applying Box–Behnken design followed by principal component analysis (PCA). CCA was further studied for its topographical, micromeritic, mechanical, compressional, and dissolution properties. Prepared CCA showed improvement in flow and packability with rich drug content (90.84%). Heckel parameters indicated greater plastic deformation ($K = 0.8132$) and tensile strength compared to the pure drug ($K = 19.256\ kg/cm^2$). CCA showed negligible elastic recovery (0.87%) compared to the pure drug (5.708%). Dissolution of the drug was increased to 2.69-folds compared to the pure drug after 60 min. No degradation or polymorphic transformation of the drug was observed even after stability study (40 °C, 75% RH). The amount of directly compressible diluents could be minimized in tablet formulation, which was a considerable improvement in the properties of the drug for making directly compressible form. The study highlights an improvement of processing characteristics of Chlorzoxazone by CCA using an integrated approach of QbD and PCA.

KEYWORDS

Chlorzoxazone; crystallo-co-agglomeration; principal component analysis; failure mode effect analysis; loading plot

1. Introduction

Majority of active pharmaceutical ingredients (APIs) available on the market belong to the BCS Class II category. The industry is facing a lot of manufacturing issues for APIs which show poor dissolution. It has also been observed that the majority of APIs having poor dissolution profiles have also shown poor flow property and compressibility.

It is very difficult to prepare solid oral dosage form with such kinds of APIs. Industry personal has to control various process and material parameters. Due to the fundamental property defects like poor physicochemical and poor mechanical properties, variability in process increases.

Quality by design (QbD) has been developed as a systematic approach for the development of a robust pharmaceutical product. It is a process to identify critical parameters involved with efficacy and safety (critical quality attributes, CQA) as well as process and materials (critical process parameters, CPP and critical material attributes, CMA) used in the manufacturing.

Drugs with poor compressibility and flowability are not suitable for direct compression. In recent times, particle engineering/design techniques are widely used in pharmaceutical industries to modify primary (particle shape, size, crystal habit, crystal form, density, porosity dust generation, etc.) as well as secondary (flowability, compressibility, compactibility, consolidation, reduced adhesion of formulation to the processing equipment, reduction in air entrapment during processing, etc.) properties of pharmaceuticals (Paradkar, Pawar, and Jadhav 2010). Especially, improvement in the efficiency of the manufacturing process and high degree of particle functionality can be achieved by these techniques. Novel techniques like pelletization (Woodruff and Nuessle 1972), fluidized bed granulation (Lachman, Liberman, and Kanig 1976), spray drying (Piera, Mara, and Etienne 2001), spray congealing (Asker and Becker 1966), melt solidification (Deshpande et al. 1997; Heng, Wong, and Chan 2000; Paradkar et al. 2003), melt sonocrystallization (Paradkar, Maheshwari, and Jahagirdar 2005), co-crystallization (Jayasankar et al. 2006), spherical crystallization (SC) (Kawashima, Okumura, and Takenaka 1982; Kawashima et al. 1984; Paradkar, Mahadik, and Pawar 1998; Chouracia et al. 2004), crystallo-co-agglomeration (CCA), etc. (Kadam, Mahadik, and Paradkar 1997a, 1997b; Yehia 2007; Paradkar, Pawar, and Jadhav 2010) have been considered as a value addition to existing ones.

Simultaneous improvement in the extent and rate of dissolution of poorly soluble drugs along with its mechanical properties is highly desirable which can lead to an increased and more reproducible oral bioavailability and subsequently to clinically relevant dose reduction and more reliable therapy (Vogt, Kunath, and Dressman 2008). Physical modification focuses on particle size reduction or generation of

CONTACT Mihir K. Raval rmihir@yahoo.com Department of Pharmaceutical Sciences, Saurashtra University, University Road, Rajkot 360 005, India.

Table 1. Quality target product profile hypothesis for CCA.

QTPP component	QTPP target	Justification
Dosage form	Directly compressible agglomerates and tablets	Directly compressible agglomerates because Chlorzoxazoneis needle/rod shaped elongated crystals which hindered the flowability and compressibility Tablet because commonly accepted unit solid oral dosage form
Route of administration	Oral	Dosage form designed to administer orally because CHL is more absorbed from the gastro-intestinal tract
Dosage strength	500 mg	Strength required for treatment
Stability	Accelerated stability of 6 months on storage condition 40 °C/75% RH	Minimum time period required (as per ICH guidance) to study stability of the final formulation
Drug product	Physical attributes	No physical defects like sticking, picking, chipping, lamination, capping, etc.

amorphous states (Hancock and Zografi 1997; Grau, Kayser, and Muller 2000).

Crystallo-co-agglomerates (CCA) are the crystals of drug aggregate in the form of small spherical particles along with excipients and solvents that were used to develop an intermediate material with improved micromeritic and mechanical properties.

Raval et al. (2013) prepared CCA of Secnidazole and improved its properties. Garala et al. (2013) formulated CCA of Racecadotril using application of principal component analysis (PCA) and DoE to explore the concept. Jadhav, Pawar, and Paradkar (2010) prepared agglomerates of bromhexine hydrochloride (BXH) with adequate sphericity and strength required for efficient tableting. Bhattacharyya, Bhattacharyya, and Patro (2010) prepared CCA of Nimesulide for direct compression. Jadhav, Pawar, and Paradkar (2007) prepared crystallo-co-agglomeration (CCA) to design directly compressible and deformable agglomerates of talc containing the low-dose drug BXH.

Various authors have worked on this formulation, but as far as the author have come across to various literature survey, no reference have been found where a combination of QbD concept with statistical design and PCA application has been used for further sorting of most influential-dependent variables in CCA formulation. In this study, CCA of model drug Chlorzoxazone are prepared using various excipients. A concept of QbD and Principle Component Analysis (PCA) are applied in the present study to explore its practical application in designing CCA followed by directly compressible tablets for beginners.

Chlorzoxazone (5-chloro-2,3-dihydro-1,3-benzoxazol-2-one), a centrally acting central muscle relaxant with sedative properties, is a poorly water soluble drug (0.2–0.3 mg/ml). It is highly cohesive powder with very poor flow property, and compressibility (Florey 1987).

2. Materials and methods

2.1. Materials

Chlorzoxazone USP was procured from Arti drugs Ltd., Mumbai, India. Klucel LF EP (HPC) and Eudragit S100 NF were gifted by Cadila Pharmaceuticals Pvt. Ltd., Dholka, India, and Evonik Degussa India Pvt. Ltd., Mumbai, India, respectively. Purified Talc was purchased from S. D. Fine Chem Limited, Mumbai, India. Ethyl cellulose Ph Eur (EC) was procured from Loba Chemicals, Mumbai, India. Polyethylene glycol 400 NF (PEG) and polyvinyl pyrrolidone K30 IP (PVP K30) were purchased from Merck Pvt. Limited, Mumbai, India, and Sisco Research Laboratories Pvt. Ltd., Mumbai, India, respectively. All other chemicals used were of analytical grade (Merck Pvt. Limited, Mumbai, India) and double-distilled water was utilized throughout the study.

2.2. Significant QTPP and CQAs

Initially, adopting an FbD-based approach of CCA development the QTPP was set-up involving a potential review of the quality features of the drug product capable of enhancing the physic-mechanical properties of Chlorzoxazone for achieving maximal therapeutic effects (Sarwar et al. 2015). The role of various elements of QTPP in developing CCA has clearly been discussed in Table 1. Similarly, Tables 2 and 3 illustrate the potential CQAs, CMAs, and CPPs affecting the performance of the CCA formulations along with suitable justification(s) for each of them, respectively.

2.3. Risk assessment

A risk assessment plan was conducted to identify the possible relations among drug and excipients with various unit operations, and estimating the probability of risk(s) or failure(s), if any (Sarwar et al. 2015). The Ishikawa fish-bone diagram was constructed to organize the risk analysis operation for determining the causes and sub-causes affecting the CQAs of drug product. Figure 1 describes the resultant fish-bone diagram depicting the effect of key material attributes and/or processing parameters for the development of CCA of Chlorzoxazone. Moreover, the prioritization exercise was carried out for selecting the factors with high risk by structuring the risk estimation matrix (REM) depicting the potential risk(s) associated with each of the material attribute(s) and/or process parameter(s) on the potential CQAs explicatively by assigning low, medium, and high values to each of them.

2.4. Selection of solvent system

The solubility study of Chlorzoxazone was carried out to select good solvent and poor solvent for drug (Raval et al. 2013).

Table 2. Critical quality attributes for CCA and their justification.

Critical Quality Attributes (CQA)	CQA target	Is this a CQA?	Justification
Drug content	More than 90%	No	Assay variability and content uniformity tend to affect drug safety and efficacy both, yet the CCA being the homogenous dispersions containing drug dispersed in the blend of excipients, these variables were regarded as moderately critical. But lower content indicated significant drug loss during crystallization
Shape	Shape and circularity factors near to 01	Yes	Spherical shape of agglomerates required for better flowability and compressibility
Flowability	Good	Yes	Better flowability required for handling, storing or processing the material
Compressibility	Good	Yes	Compressibility is an important approach in practice is the focus on the manufacturing of tablets with adequate strength
Crushing Strength	More than 50 g	Yes	Good strength of agglomerates required for improvement in mechanical and handling properties
Assay	More than 95 %	No	As it is must to meet the compendial standards (95–105% of label claims), this factor is considered as less critical
Suitable for storage of the final dosage form	In aluminum strip	No	To retain product integrity and quality up to target shelf life. As drug is a stable molecule, this factor is considered as less critical

Table 3. Critical material attributes (CMA) and critical process parameters (CPP) for CCA and their justification.

Critical Processing and Material Attributes (CPP and CMA)	CPP/CMA	Justification
Speed and type of stirrer	CPP	Optimized speed of stirrer is needed to start agglomeration of recrystallized particles. Higher speed may break the particles too. Baffle type is more suitable
Ratio of good solvent: poor solvent		Initiation of crystallization and sufficient crystal generation depends on ratio of Good: Poor solvents.
Mean time observation of CCA formation		Observation at different time interval in microscope is required to confirm the agglomeration as well as to stop stirring
Temperature of poor solvent		Initiation of crystallization and sufficient crystal generation depends on temperature of poor solvent also
Type of material	CMA	Polymers are required to control the crystal growth, shape of particle and binding of crystals together in order to convert bunch of crystals in to agglomerates
Concentration		Proper concentration is required to shape of particle and binding of crystals together in order to convert bunch of crystals in to agglomerates
Solubility in solvents		Polymers should be soluble in either of the solvents which ultimately gets recrystallized with drug. Some may act as seed.
Quality of excipients		Good quality excipients are required as per the pharmacopeial standards

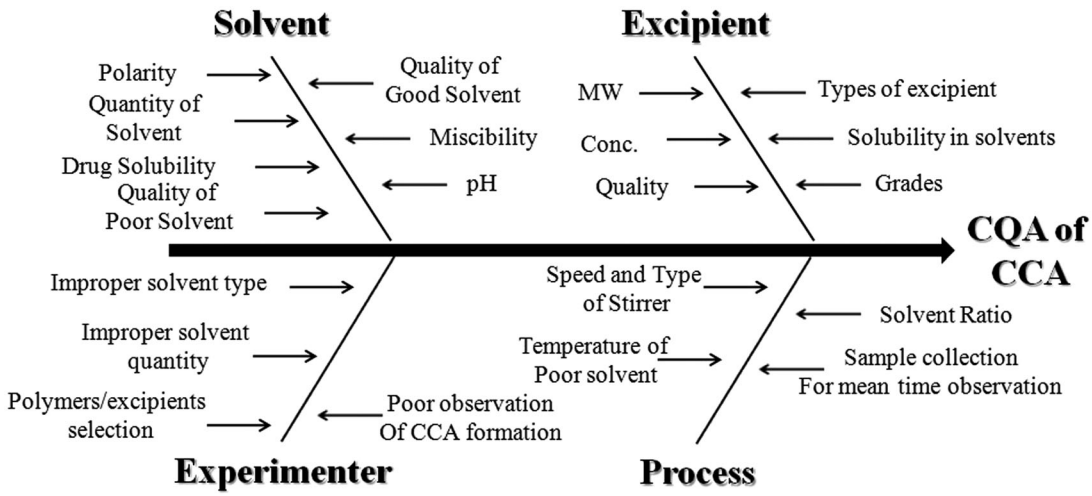

Figure 1. Ishikawa fish-bone diagram.

A range of solvents from highly polar to non-polar nature were selected and solubility of pure drug was checked. About 5 ml of each solvent was taken and an excess amount of drug was added in it. These saturated solutions were then kept for 24 h in Cryostatic constant temperature reciprocating shaker bath (Tempo Instrument Pvt. Ltd., Mumbai, India) at the temperature of 25 ± 1 °C with continuous shaking at 120 RPM. The saturated solutions were then filtered using 0.45 micron whatman filter paper (previously soaked with individual solvents) and amount of drug dissolved in particular solvent was

measured at 280 nm using UV–Visible Spectrophotometer (Pharmspec 1800, Shimadzu, Japan). The study was in triplicate in the same manner to obtain reproducible results.

2.5. Selection of influential factors by failure mode effect analysis (FMEA)

An overall assessment of risk was studied by the failure mode effect analysis (FMEA) as per the ICH Q9 guideline. It is required to find out the factors which can destroy the overall process of making CCA. FMEA identifies and prioritizes the factors of product or process and its serious effect resulting in to failure of the overall formulation, frequency of its occurrence, how easily they can be detected (Fahmy et al. 2012). Factors can be ranked according to the Risk Priority Number (RPN). Factors which have very high impact on failure of the product can be shortlisted using RPN and can be studied further. The factors which are having low impact are not required to study further. RPN was calculated using the following equation:

$$\mathrm{RPN} = \begin{pmatrix} 5 \\ 4 \\ 3 \\ 2 \\ 1 \end{pmatrix} \mathrm{O}\ \mathrm{X} \begin{pmatrix} 5 \\ 4 \\ 3 \\ 2 \\ 1 \end{pmatrix} \mathrm{S}\ \mathrm{X} \begin{pmatrix} 1 \\ 2 \\ 3 \\ 4 \\ 5 \end{pmatrix} \mathrm{D} \qquad (1)$$

Here, O is the probability of occurrence or chances to occur a particular event; we ranked it as 5 (frequently happening); 4 (probable happening); 3 (occasionally occurring); 2 (rarely occurring) and 1 (improbable to occur). The next parameter S is the severity, which is a measure of how severe is it so that the failure will happen; we ranked these as 5 (terrible); 4 (significant); 3 (serious); 2 (rare) and 1 (negligible or no effect). The final parameter D is the ability to detect. It means that how easily we can detect the chances of failure due to a particular factor. Hence, ease of detection of a factor which can cause failure, may become less critical to the product quality. For D, we ranked 1 (easily detectable); 2 (detectable); 3 (reasonably detectable); 4 (low detectability) and 5 (tough to detect). For the sake of selecting critical factor, the RPN numbers were ranked as, RPN less than 30 was less risky, RPN more than 30 and less than 50 was moderate risky and RPN equal or more than 50 was of high risk. In such case, factors having RPN equal or more than 50 were required to study further for controlling/optimizing those to obtain successful product.

2.6. Preparation of agglomerates (CCA)

On the basis of solubility study, good and poor solvents were identified and selected for the preparation of CCA. A crystallization protocol was designed in which the drug and/or single or combination of excipients in different ratios were dissolved in good solvent and added drop wise to the bad solvent which was being stirred by using four blade mechanical stirrers (Remi Motors Ltd., Mumbai, India) (Raval et al. 2013). Here, the good solvent also acted as a bridging liquid. The stirring was continued for some time. The stirring was stopped when the overall mixture appeared clear at the top and the particles settled down. The agglomerates generated were filtered and dried at room temperature. The surface moisture was removed by storing the samples in the desiccators containing self indicating silica crystals for 1–2 weeks and stored in an air tight screw cap glass bottle.

2.7. Box–Behnken experimental design

Box–Behnken statistical screening design was applied to evaluate main effects and interaction effects of independent factors on the various properties of Chlorzoxazone CCA to optimize the formulation (Chopra et al. 2007). The non-linear quadratic model generated by the design is as follows:

$$Y_i = b_0 + b_1X_1 + b_2X_2 + b_3X_3 + b_{12}X_1X_2 + b_{13}X_1X_3 + b_{23}X_2X_3 + b_{11}{X_1}^2 + b_{22}{X_2}^2 + b_{33}{X_3}^2 + b_{123}X_1X_2X_3 \qquad (2)$$

where Y_i is the dependent variable, b_0 is the arithmetic mean response of 13 runs and b_i represents the estimated coefficient for factor X_i. X_1, X_2, and X_3 are the main effects having the value from lowest to highest along with the coded value −1 to +1. It gives an average result of altering one factor at a time from its lowest to highest value. The interaction terms (X_1X_2, X_2X_3, X_1X_3, and $X_1X_2X_3$) represent change in responses when two or three factors are simultaneously changed. The polynomial terms (${X_1}^2$, ${X_2}^2$, and ${X_3}^2$) are added to investigate non-linearity of the model (Maurya et al. 2011). A three-factor, three-level Box–Behnken design was applied by an experimental design software Design-Expert trial version 7.1.5. Based on preliminary trials and risk analysis by FMEA, independent variables (factors), which represented maximum RPN value (equal to or more than 50), were determined as: Concentration of polymers PVP K30, PEG 400, and ethyl cellulose as X_1, X_2, and X_3, respectively. Additionally the composition of optimized (check point) batch was derived by constructing overlay plot. The percentage relative error of each response was calculated using following equation in order to judge validity of the model (Garala et al. 2013).

2.8. Packability and flow parameters

For the rheological characterization of the prepared samples, angle of repose, Carr's index, and Hausner's ratio were measured. Angle of repose was determined using fixed funnel method (Fernádez-Arévalo, Vela, and Rabasco 1990; Aulton 2007). Percentage compressibility (Carr's Index) and Hausner's ratio were calculated after tapping of fixed amount of sample using Electrolab tap density tester (USP) (Lachman, Libermann, and Kanig 1991). Angle of repose (α) of the powder material was calculated using the following formula:

$$\alpha = \tan^{-1}(h/r) \qquad (3)$$

where h is the height of the pile and r is the radius of the pile (Martin, Swarbrick, and Cammarata 1991).

The bulk density (ρ_b) was the quotient of weight to the volume of the sample at zero tap. Tapped density (ρ_t) was determined as the quotient of weight of the sample to the volume after tapping a measuring cylinder for 500 times from a height of 2 inch. Carr's Index (percentage compressibility—CI) was calculated as one hundred times the ratio of the difference between tapped density and bulk density to the tapped density:

$$\text{CI } (\%) = \frac{\rho_t - \rho_b}{\rho_t} \times 100 \tag{4}$$

Hausner's ratio (HR) was calculated using measured values of bulk density and tapped density as follows:

$$\text{HR} = \frac{\rho_t}{\rho_b} \tag{5}$$

Packability parameters like a (compressibility, or amount of densification due to tapping), $1/b$ (cohesiveness, or how fast/easily the final packing state was achieved), and K (Kuno's constant was determined directly putting the values of densities) were calculated using Kawakita and Kuno's equations at taps 10, 30, 50, 100, 200, and 300 (Raval et al. 2015).The values of "a" and "b" were calculated from the slope and intercept of the linear plot of N/C Vs N, respectively.

2.9. Kawakita equation

$$\frac{n}{C} = \frac{1}{ab} + \frac{n}{a} \tag{6}$$

Here, $Y = N/C$, slope $= N/a$, and intercept $= 1/ab$, where, $C = \frac{(V_0 - V_n)}{V_0}$ (Patra et al. 2007).

2.10. Kuno's equation

$$ln(\rho_t - \rho_n) = -Kn + ln(\rho_t - \rho_o) \tag{7}$$

where n is the number of tapping; V_0 and V_n are the initial volume and the volume after "n" no. of taps; q_0, q_n, and q_t are the initial density, density at "n" taps and density at infinite taps respectively; a, b, and K are the constants representing flowability and packability of powder under mechanical force.

The smaller values of parameters "a" and "$1/b$" in Kawakita equation for the samples indicated higher packabilities of the sample compared to pure drug. Higher values of parameter "K" in Kuno's equation for sample were an indication of marked improvement in compressibility and packability attributed to the much higher rate of their packing processes than that of pure drug due to sphericity of particles (Patra et al. 2007).

2.11. Capillary melting point

The sample was filled in one end sealed capillary and melting range was determined on digital melting point apparatus (accuracy ± 0.1 °C).

2.12. Microscopic determination and surface topography

The shape and size of the samples were observed under the optical microscope with 10× magnification and photomicrographs were taken using CCD camera for comparing morphological changes in prepared samples compared to pure drug. The preliminary observation of the shape and surface of the prepared samples was done and the batches for the further study were selected.

2.13. Drug loading efficiency and % yield

Drug loading efficiency is the ratio of experimentally measured drug content to the theoretical value, expressed as percentage (%) (Chaulang et al. 2008; Chavda and Maheshwari 2008).

Accurately weighed quantity of prepared samples were dissolved in little quantity of a suitable solvent in which it was easily soluble and made the volume to 50 ml in a volumetric flask. These solutions were appropriately diluted and drug content was determined by UV spectrophotometer using the same solvent as blank. The experimental drug content was calculated using calibration equation. The % yield of sample was calculated using the following formula:

$$\%\text{Yield} = \frac{\text{total weight of sample}}{\text{total weight of drug and polymer}} \times 100 \tag{8}$$

2.14. Micromeritic study

The size analysis was performed using optical microscopy method. The size and size distribution of particles were counted using eye piece micrometer which was previously calibrated using stage micrometer. The particle size was determined by taking longest dimension of the particle for a minimum of 100 particles. Mean aspect ratio (AR), defined as the ratio of length (longest dimension from edge to edge of a particle oriented parallel to the ocular scale) to the width (the longest dimension of the particle measured at right angles of the length) of the particle, was calculated (Banga et al. 2007; Kumar, Chawla, and Bansal 2008). The size of 300 randomly selected particles from prepared batch was measured and appropriate geometric mean diameter (d_g) was calculated (Martin, Swarbrick, and Cammarata 1991).

2.15. Sphericity determination

Shape factor (SF) and circularity factor (CF) for the prepared sample were obtained from the area (A) and perimeter (P') of the particle (Chandresh, Malay, and Prajapati 2018). The photomicrographs of the particles were taken at

40× using CCD camera and tracings of the enlarged photomicrographs were used for the measurement of area and perimeter:

$$SF = \frac{P'}{P} \quad (9)$$

Where $P' = 2\pi\ (A/\pi)^{1/2}$

$$CF = (P')^2/4\pi A \quad (10)$$

2.16. Crushing strength

The crushing strength of the prepared sample was determined by mercury load cell method using 10 ml hypodermic glass syringe (Chatterjee, Gupta, and Srivastava 2017). The particle was placed inside the syringe and mercury was added through hollow syringe tube. The total weight of tube with mercury, at the stage where particle broke, gave the measure of crushing strength of that particle.

2.17. Heckel plot

Accurately weighed quantity of prepared samples was compressed at the constant compression at different pressures (Maghsoodi et al. 2008). The punch and die were lubricated using 1% w/v dispersion of magnesium stearate in acetone. The compression behavior of the samples was expressed as parameters of Heckel equation (Autamashih et al. 2011). Plot of ln [1/(1 − D)] versus P was drawn and values of K, A and σ_0 were obtained:

$$ln\frac{1}{1\ -\ D} =\ kP\ +\ A \quad (11)$$

where D is the relative density of compacts, that is, ratio of compact density to true density of powder, P is the applied pressure, K is the slope of Heckel plot; $K = 1/P_y$. P_y is the mean yield pressure. The constant A expresses the densification at low pressure. σ_0 is yield strength, $\sigma_0 = 1/3\,K$.

Here, the density of prepared compacts for Heckel parameter was calculated from volume of compacts and mass of compacts.

2.18. Tensile strength measurement

After the determination of diameter and thickness of compacts prepared for the study of Heckel parameters, the compacts were subjected to relaxation for 24 h. Then the compacts were subjected to tensile strength measurement in which the force required to break the compacts (P) was measured using Monsanto hardness tester (Raval et al. 2013). The tensile strength (T, kg) of the compacts was calculated using the following equation (Thapa et al. 2019):

$$T = \frac{0.0624 \times P}{D \times L} \quad (12)$$

where D and L are the diameter and the thickness (cm) of the compacts, respectively. P is the force (kg/cm^2) required to break compacts.

2.19. Elastic recovery

The compacts prepared for the Heckel plot study and tensile strength determination were used for the elastic recovery test. The thickness of the compacts was measured immediately after ejection (H_c) and after the 24 h relaxation period (H_e). The elastic recovery was calculated using the equation (Armstrong and Haines-Nutt 1974):

$$\%\ ER = [(He - Hc)/\ Hc] \times 100 \quad (13)$$

2.20. Differential scanning calorimetry

Thermograms of the pure drug and prepared samples were performed using DSC-60 (Shimadzu, Tokyo, Japan) calorimeter to study the thermal behavior of drug and prepared samples (Patel et al. 2019). The instrument comprised of calorimeter (DSC 60), flow controller (FCL60), thermal analyzer (TA 60 WS), and operating software (TA 60). The samples were heated in hermetically sealed aluminum pans under air atmosphere. Empty aluminum pan was used as a reference.

2.21. Fourier transform infrared (FT-IR) spectroscopy

Infrared spectra of pure drug and prepared samples were recorded using infrared spectrophotometer (FTIR 8400 spectrophotometer, Shimadzu, Japan) (Patel et al. 2019). The samples were dispersed in KBr and compressed into disc/pellet by application of pressure. The pellets were placed in the light path for recording the IR spectra. The spectrum was recorded.

2.22. Powder X-ray diffractometry

The X-ray powder diffraction patterns of pure drug and optimized samples were recorded using PANalytical diffractometer system (Xpert pro PW 30-40/60) with a copper target and scintillation counter detector (voltage 40 kV; current 30 mA; scanning speed 0.05°/sec). The sample holder was non-rotating and temperature of acquisition was room temperature. The diffraction pattern was analyzed in a specific 2θ range (Patel, Raval, and Sheth 2020).

2.23. Scanning electron microscopy

The shape and surface morphology were observed using scanning electron microscope (JEOL, JSM 5610 LV, Tokyo, Japan). The samples were observed at various magnifications to have an idea about the effect of various additives on surface treatment (morphology) and particle size (Patel, Raval, and Sheth 2020).

2.24. Moisture content

Moisture content of agglomerates was measured in Hot air oven (Janki Impex Pvt. Ltd., Ahmedabad, India). Agglomerates (5 g) were placed in the heating chamber of

the instrument and heated constantly at 105 °C for 4 h. The percent reduction in the weight of agglomerates due to moisture loss was measured by measuring the weight of the agglomerates after heating. Difference in weight of agglomerates before and after the treatment was a measure of percentage moisture content in agglomerates. The study was performed in triplicate.

2.25. Preparation of directly compressible tablets

Formulation excipients were selected on the basis of preliminary tests which demonstrated no interference of these excipients at the λ_{max} of API. Tablets containing equivalent amount of API were made by direct compression using different formulation excipients of directly compressible type. Samples used for tableting were having similar size range of particles. The material for each tablet was weighed (containing equivalent amount of API), introduced manually into the die and compressed in tablet machine. The compaction surfaces were lubricated with 2% w/w magnesium stearate in acetone before compaction. The blend was compressed on an eight-station rotary tablet machine (Karnawati Engineering Ltd., Ahmedabad, India) to obtain tablets of required hardness and thickness. The tablets were studied in three replicates. The compacts were ejected and stored in screw-capped bottles for 24 h before using, to allow for possible hardening and elastic recovery. The compacts were also taken for in-process and finished product evaluation tests. The same technique was applied for preparation of tablets of API as well as tablets of control batch.

2.26. Evaluation parameters for prepared directly compressible tablets

2.26.1. Thickness and diameter of the tablets

The thickness and the diameter of individual tablet were measured with a Vernier caliper, which permitted accurate measurements. The study was conducted for 20 tablets and average result was considered.

2.26.2. Weight variation test of the tablets

The USP has provided limits for the average weight of uncoated compressed tablets. Twenty tablets were weighed individually and the average weight was calculated.

2.26.3. Tablet friability test

Tablet friability was measured by using Roche friabilator (Electrolab, Mumbai, India). Ten tablets were weighed and placed in the apparatus where they were exposed to rolling and repeated shocks as they fall 6 inches in each turn within the apparatus. After 4 min of this treatment or 100 revolutions, tablets were weighed and compared with the initial weight. The loss due to abrasion was a measure of the tablet friability.

2.26.4. Tablet hardness test

Tablet hardness was measured using the Pfizer hardness tester. The instrument measured the force required to break the tablet when force generated by a coil spring was applied diametrally to the tablet. The test was done for three tablets from each samples and average was considered.

2.26.5. Tablet disintegration test

The disintegration test is a measure of the time required under a given set of conditions for a group of tablets to disintegrate into particles which will pass through a 10 # screen. The disintegration test was carried out using the tablet disintegration tester (Electrolab, Mumbai, India) which consisted of a basket rack holding 6 plastic tubes, opened at the top and bottom, the bottom of the tube was covered by a 10 # screen. The basket was immersed in 1 l beaker containing distilled water held at 37 ± 1 °C. As the basket was moved up and down, tablets kept in the tubes were started disintegrating. The time required for disintegration of tablet was measured in accordance with the United States Pharmacopeia 29.

2.27. In vitro dissolution of prepared samples and dosage form

A USP dissolution test apparatus were used to monitor the dissolution profiles to evaluate the influence of process and excipients on drug release. The dissolution medium was equilibrated to 37 ± 0.5 °C. Peddles/baskets were rotated at predetermined RPM. From the dissolution flask, 5 ml samples were withdrawn at selected time intervals (Hector et al. 2000) and the concentrations of API in the samples were determined by UV spectrophotometer at λ_{max} of drug by diluting with suitable solvent using same media as blank. The mass of API dissolved was calculated from the concentration after correcting for the change in volume of the dissolution medium. The concentration of drug was calculated by fitting value of absorbance read in the linear regression equation for the calibration curve of drug at its λ_{max}. All determinations were performed in triplicate.

2.28. Dissolution parameters

The dissolution data were analyzed by model independent parameters calculated at different time intervals, such as dissolution percent (DP), dissolution efficiency (%DE), and time to release 50% of the drug (t50%). DP at different time intervals and t50% can be obtained from percent dissolution vs time profile/data (Zaborenko et al. 2019).

Dissolution efficiency is a parameter for the evaluation of *in vitro* dissolution data. Dissolution efficiency is defined as the area under curve (AUC) up to a certain time "*t*" expressed as percentage of the area of the rectangle described by 100% dissolution in the same time (Anderson et al. 1998).:

$$\%DE = \int_0^t \frac{y.dt}{y_{100}t} \times 100 \tag{14}$$

2.29. PCA

PCA was implemented to identify grouping of the materials using The Unscrambler®10.2 software (trial version) (CAMO AS, Norway). The data matrix included the number of batches as per the predefined rule set (total runs, = 13 + 01 for pure drug), each characterized by 15 dependent variables. PCA model was performed using methodical treatment to data (Garala et al. 2013). An organized approach was applied; first, including pure drug and agglomerates into the model, followed by recognition of extremes or possible outliers. These outliers were then omitted to study remaining variables for further analysis.

2.30. Stability study

The optimized batch was placed in 20 ml borosilicate glass ampoule. The mouth of the ampoule was closed tightly with aluminum foil to prevent the access of air from the atmosphere to the sample inside the ampoules. Six such samples were stored at 40 °C and 75% relative humidity (RH) for 3 months. The dissolution behavior of samples and dosage forms was evaluated in triplicate and characterized (Zhang et al. 2010).

3. Results and discussion

3.1. Risk assessment

Figure 1 depicts the Ishikawa fish-bone diagram for the CCA shows a cause-and-effect relationship among the probable factors influencing the drug product CQAs. Tables 1–3 illustrate the risk assessment matrix suggested for identifying the QTPP and also risk associated with each material attributes and/or process parameters. Rational justification of various risk(s) for each of the material attributes and process parameters corresponding to the respective CQAs is enlisted in these matrixes.

3.2. Selection of solvent system and formation of CCA

From Table 4, it was observed that Chlorzoxazone exhibited good solubility in di-methyl formamide and acetone. At the same time, it showed poor solubility in distilled water as well as hexane. Hence, former were selected as good solvents and later were selected as poor solvents for the maximum recrystallization of drug. The drug was dissolved in good solvent (DMF or acetone) and added drop wise to the bad solvent (water or hexane) which was being stirred by using four blade mechanical stirrers. The amount of good solvent was 10 ml and poor solvent was 200 ml and this ratio was kept constant in all the trials. Excipients used in the preparation of agglomerates were PVP K30, PEG 400, Eudragit S100, HPC LF, EC, Purified talc, etc., which were co dissolved either in good or poor solvents alone or in combinations.

The study revealed poor or negligible agglomeration in absence of additives (control batch). Preliminary trials were conducted with various excipients in various concentrations ranging from 0.2% to 2.0% w/v of the saturated solution of drug in acetone-distilled water or DMF-distilled water system. In most of the cases, agglomerates could not be formed. The solution of drug excipients in acetone as good solvent was added drop wise into poor solvent like hexane with constant stirring started little agglomeration. The combinations of various excipients were also used where the concentration of one was kept constant (which gave good results at that particular concentration) while varying concentration of second excipient. The agglomerates obtained in preliminary trials were subjected to the evaluation of angle of repose, Carr's index, Hausner's ratio, Kawakita, shape factor, circularity factor, and crushing strength (data not shown as preliminary trials). Some batches were rejected during preliminary trials. Although the presence of excipient(s) improved the flow of the co-agglomerates as compared to pure drug and control batch, significant results were not found with all the additives. Various combinations of the additives were also tried and not all but some of them produced co-agglomerates with remarkable improvement in micromeritic and mechanical properties.

Moreover, agglomerates were also prepared at various stirring speed ranging from 100 to 600 RPM on mechanical stirrer (Remi Laboratory Instruments, Mumbai, India). All the batches were evaluated based on the crushing strength of agglomerates (Table 5). The results revealed that at 100 and 200 RPM, no agglomerates were formed. Produced shear energy might not be sufficient for the formation of CCA. Probably low stirring speed was not sufficient to generate a centrifugal effect over the recrystallized drug-excipient mixture in the solution (Garala et al. 2013). At 300 RPM, agglomerates showed poor crushing strength. Good results with sufficient crushing strength were obtained in case of 400 RPM. Above that, again there was a reduction in crushing strength. It might be due to unwanted higher impact energy of collision was generated by stirrer. Moreover, it might cause destruction of forming agglomerates (Bose et al. 2011). Hence, 400 RPM was kept as constant for the entire preparation.

Table 4. Solubility of chlorzoxazone in various solvents.

Sr. no.	Solvent	Solubility (mg/ml) Mean ± S.D.[a]	Sr. no.	Solvent	Solubility (mg/ml) Mean ± S.D.[a]
01	Ethanol	257.88 ± 0.031	09	Cyclohexane	59.88 ± 4.61
02	Hexane	0.58 ± 0.509	10	Octanol	30.61 ± 0.012
03	Propanol	266.67 ± 0.350	11	Pet. Ether	10.58 ± 0.031
04	DMF	486.67 ± 4.140	12	Chloroform	5.75 ± 0.015
05	Methanol	351.52 ± 0.764	13	DCM	5.42 ± 0.011
06	Ethyl Acetate	336.36 ± 0.382	14	Toluene	3.09 ± 0.052
07	Acetone	216.06 ± 2.22	15	CCl4	0.78 ± 0.041
08	n-Butanol	114.55 ± 0.127	16	Distilled water	0.21 ± 0.063

[a]Each reading is mean ± S.D. of three readings.

Table 5. Optimization of speed of rotor in CCA formation.

Sr. no.	RPM	CCA formation	Crushing strength ± S.D.[a]
1	100	Only Fines generated	NA
2	200	Only Fines generated	NA
3	300	CCA formed with bigger size	35.26 ± 1.275
4	400	CCA formed	51.32 ± 2.051
5	500	CCA formed	42.53 ± 1.391
6	600	CCA formed and starts breaking	40.31 ± 1.227

[a]Data expressed as mean ($n = 3$).

On the bases of above trials, it was really necessary to explore the influential factors using Risk analysis and FMEA which could really affect the formation of CCA.

3.3. Failure mode and effect analysis (FMEA)

For FMEA, Table 6 enlists the factors that were believed in development of CCA while executing FMEA. In the present study, the RPN ≥50 was considered as high risk, ≥30 to <50 was considered as medium risk, and <30 was considered as low risk (Vora et al. 2013). From Table 6, it is obvious that RPN of polymers/excipients such as PVP K30, EC and PEG 400 RPN were 75, 60, and 75, respectively, and needed thorough analysis. Thus, their optimization was done using response surface method for establishing design space. Selection of good and poor solvents as well as amount of Eudragit S100 were at moderate risk. The amount of good and poor solvents, stirring speed, and duration of stirring were at low risk category. Initial risk assessment studies using aforementioned tools have recommended that three factors, that is, amount of polymers/excipients such as PVP K30, EC, and PEG 400 were found to be highly critical due to the high risk associated with them on CQAs and explored further using Design of Experiment.

3.4. Box–Behnken design

After conducting various evaluation studies of preliminary batch and from the extract of FMEA, Box–Behnken design was selected. Finally, concentration of PVP K30 (X_1), PEG 400 (X_2), and EC (X_3) were selected as independent variables. Further levels were also selected. Selection of linear co-relation with two levels was somewhat confusing, hence, three levels were chosen to get linear co-relations. Thus, as per the design matrix, total 13 batches were prepared. The three levels (−1, 0, +1) were selected for all the factors by keeping their concentration different (Chopra et al. 2007). The levels and design is given in Table 7. For all experimental design batches of CCA, responses like, mean geometric diameter (dg), crushing strength (CS), shape factor (SF), Carr's index (CI), percent yield (%Y), drug content (DC), circularity factor (CF), Hausner ration (HR), angle of repose (AoR), Kawakita parameters ($1/b$), Kuno's constant(K), Heckel plot parameter (k), elastic recovery (ER), tensile strength (TS) and moisture content (MC) were evaluated and documented in Table 8.

3.5. PCA

PCA is a statistical algorithm that reduces the dimensionality of the data while retaining most of the deviation in the data set (Thapa et al. 2019). PCA is used for getting general idea of data tables (their arrangement, similarities or dissimilarities, tendencies, deviating observations). Initially, PCA was executed to observe the relationship of all dependent variables obtained from the series of experimental design and control batch of CCA. Further, identification of objects was carried out by investigating from the score plots (Figure 2) and the loading plots (Figure 3). The loading plot depicts the behavior of various dependent variables to the principal components and the score plot depicts the behavior of various batches prepared from experimental design. As depicted in Figure 2(B), the first two principal components were able to explain 64% (PC1) and 14% (PC2), respectively, totally 78% of the variation in the data. Design batches and dependent variables located on the same side and the same direction of the co-ordinate system formed by the principal components (PCs) are positively correlated, while those placed diagonally on the two sides of the origin are inversely correlated. In the score plot shown in Figure 2, the data show a distinct grouping related to the different excipients. Based on the PCA score plot in Figure 2(A), pure drug was sorted as insignificant objects due to outside of eclipse. Pure drug was eliminated from the data set and a new PCA model was built without pure drug to better demonstrate the allocation of the remaining batches of design for agglomerated Chlorzoxazone. The PCA score plot of all the variables of 13 batches of Box–Behnken design is given in (Figure 2(B)). The score points spread out relatively homogeneously into four quartiles of the score plot. As seen from Figure 2(B), all the formulations were clustered into five groups: group I (batch nos. 7, 11, and 12), group II (batch nos. 2, 3, 6, 9, and 10), group III (batch nos. 1 and 5), group IV (batch no. 8), and group V (batch nos. 4 and 13). All the five groups were relatively distant and substantially different from one another.

The loading plot (Figure 3) indicates that which of the dependent factors is indicative of the grouping. The variables CI, AoR, and drug content along with CS are positively correlated along PC1 and inversely correlated to $1/b$ and %Y along the same PC. At the same time, $1/b$ and %Y are positively correlated along PC1. Loading plot given in Figure 3(A), where the values of parameters of pure drug were considered with the contribution of PC1 and PC2 were 77% and 14%, respectively (Haware, Tho, and Bauer-Brandl 2009). In this plot also, pure drug was sorted as insignificant object, it was omitted and constructed as Figure 3(B). From Figure 3(B), it was clearly observed an improvement of dependent variables, where CI, AoR are positively correlated with each other. Spherical or rounded particles pack more closely than flat or elongated particles, they have less interparticular spaces, and show better flowability (Raval et al. 2013). At the same time, $1/b$ and CS are oppositely correlated with each other. Rest of the factors was clubbed at center, hence, not discussed.

Correlation loading plot was also constructed to decide most significant dependent variables for further optimization. Correlation loading plot shown in Figure 4 represents the five most significant dependent variable (marked by a dotted circles) as they enclosed between two eclipse (Thapa et al. 2019). There was a highest batch to batch variation in the result of those dependent variables; hence, it was required to study the behavior of those variables through application of response surface methodology for further analysis to get optimized CCA.

Table 6. Calculation of risk priority numbers (RPN) for the formulation of CCA.

Formulation/process parameter component	Failure mode	Failure effects	S_a	Potential causes or root of failure	O_b	Detection or control method	D_c	RPN
Selection of Good Solvent	Solubility of drug and other excipients	No CCA formation/ Very poor CCA	5	Improper Drug solubility study	3	Multiple time study, accuracy, UV detection	3	45
Selection of Poor Solvent	Inadequate crystallization of drug and other contents		5		3		3	45
Amount of Good solvent	Less content dissolved	More fines generated, Agglomerates size, Strength	5	Operator's error	2	Sieve analysis, Crushing strength apparatus	3	30
Amount of Bad solvent	Improper re-crystallization	More fines generated, Agglomerates size	5	Operator's error	2	Sieve analysis	3	30
PVP K30	Improper concentration	Poor binding, Improper shape, Poor Mechanical strength	5	Operator's error	5	Shape analysis, Crushing strength measurement	3	75
Eudragit S100	Improper concentration	Poor Mechanical strength	3	Operator's error	5	Crushing strength measurement	3	45
EC	Improper concentration	Improper shape, Poor Mechanical strength	4	Operator's error	5	Shape analysis, Crushing strength measurement	3	60
HPC LF	Improper concentration	Poor binding or lump formation	3	Operator's error	5	Crushing strength measurement	2	30
HPMC E50LV	Improper concentration	Poor Binding/Lump formation	5	Operator's error	5	Visual observation	2	50
Talc	Improper concentration	Poor seeding or poor dissolution rate	5	Operator's error	2	Dissolution study/opaque solution	2	12
Agglomerating agent (PEG 400)	Improper concentration	Poor Mechanical strength	5	Operator's error	5	Crushing strength measurement	3	75
Stirring speed	Un-optimized Stirrer speed	Poor agglomerates shape and size	3	Operator's error, equipment failure	3	Shape and sieve analysis	2	18
Duration of stirring	Inadequate time of processing	Incomplete crystallization, Poor mechanical strength, size	4	Operator's error	3	Crushing strength measurement	2	24

Table 7. Variables in Box–Behnken design for CCA formulation.

	Independent variables		
Batch code	X_1	X_2	X_3
1	−1	−1	0
2	1	−1	0
3	−1	1	0
4	1	1	0
5	−1	0	−1
6	1	0	−1
7	−1	0	1
8	1	0	1
9	0	−1	−1
10	0	1	−1
11	0	−1	1
12	0	1	1
13	0	0	0

	Levels		
Factors	−1	0	+1
X_1 (concentration of PVP K30; %W/V)	0.5	1.25	2
X_2 (concentration of PEG 400; %W/V)	0.2	1.1	2
X_3 (concentration of EC; %W/V)	0.2	1.1	2

3.6. Response surface methodology

For all the 13 batches of experimental design, the data clearly indicated strong influence of independent factors (X_1, X_2, and X_3) on selected responses. The polynomial equations were used to draw conclusions after considering mathematical magnitude of coefficients by considering the maximum level of significance within 5% (Chopra et al. 2007). For Angle of repose (AoR), all the factors except X_3 were insignificant. Moreover, coefficient value of X_3 showed positive correlation (2.43). It was an indication that amount of ethyl cellulose had a profound influence over the formation of CCA, particularly flow of agglomerates. Though from regression analysis, it was observed that X_2 was an insignificant factor; Figure 5(A) suggests that as the amount of PEG 400 increased, AoR decreased. It might be due to a sphericity enhancing capability of PEG 400 (Jakob 2006; Manoj et al. 2019). Similar regression behavior was also calculated for Carr's Index (Figure 5(B)) and Crushing strength (Figure 5(C)). It was noticed that, in both the cases, CI and CS were increasing with the increase in the concentration of PVP K30 and PEG 400. Both the excipients were responsible for sphericity enhancement as well as binding more amounts of drug crystals in the slurry (Jakob 2006; Manoj et al. 2019). It could alter the crystal habit and imparted spherical shape by adsorbing at the growing surface and controlling or blocking the rate/growth of crystal formation (Sekikawa, Nakano, and Arita 1978; Ring 1991; Ribardière et al. 1996; Pawar et al. 2007). Due to these properties, there was an increase in flow and mechanical strength of CCA. At the same time, the amount of EC also played a vital role in improving strength of CCA (Raval et al. 2013). In case of circularity factor (CF), it was noticed that, as concentration of PVP and PEG increased, the value of CF was increased followed by reduction (Figure 5(D)). This behavior was due to the presence of PEG, which could provide a smooth surface to agglomerates (Jakob 2006). Further increase in PVP K30 concentration could have increased stickiness in system which leads to improper agglomerate formation and reduction in the value of CF (Deshkar et al. 2017). From regression analysis, it was found that all the significant factors were inversely proportional to CF (negative coefficient values). EC apart from strength improvement generated surface roughness, hence, reduction in AoR as well as CF (Pawar et al. 2004). In case of geometric mean diameter (dg) (Figure 5(E)), it was found that all the coefficient values of significant factors were directly proportional to it. It would be expected that the viscosity of the polymer mixture would increase as polymer concentration rose, resulted in enhanced interfacial tension and hence, formation of larger particles (Garg and Gupta 2010). Following are the regression equations:

$$AoR = 18.41 + 0.29X_1 - 1.395X_2 + 2.43\ X_3 + 0.495\ X_1X_2 + 0.225\ X_2X_3 - 1.41X_1X_3 + 1.405\ X_1{}^2 + 1.685X_2{}^2 + 3.92X_3{}^2 (R^2 = 0.9375) \quad (15)$$

$$CI = 14.7 + 0.76X_1 + 0.8225X_2 + 2.4475\ X_3 - 1.2325\ X_1X_2 + 0.7225\ X_2X_3 - 0.4825X_1X_3 + 0.8287\ X_1{}^2 + 0.7038X_2{}^2 + 2.5188\ X_3{}^2 (R^2 = 0.9087) \quad (16)$$

$$CS = 46.27 + 3.28X_1 + 2.071X_2 + 3.72X_3 - 0.2725X_1X_2 - 0.345X_2X_3 - 0.0375X_1X_3 - 2.26X_1{}^2 - 2.45X_2{}^2 + 2.11X_3{}^2 (R^2 = 0.9336) \quad (17)$$

$$CF = 1.055 + 0.00381X_1 + 0.0145X_2 - 0.06211X_3 + 0.00703X_1X_2 - 0.01658X_2X_3 - 0.01375X_1X_3 - 0.3518X_1{}^2 - 0.01835X_2{}^2 - 0.1521X_3{}^2 (R^2 = 0.9947) \quad (18)$$

$$dg = 1.009 + 0.08675X_1 + 0.136X_2 + 0.1213X_3 + 0.02825X_1X_2 - 0.03625X_2X_3 + 0.02276X_1X_3 - 0.2966X_1{}^2 - 0.2166X_2{}^2 + 0.03438X_3{}^2 (R^2 = 0.9788) \quad (19)$$

From the overlay plot (Figure 5(F)), Check Point Batch was prepared. From the equation, it was confirmed to have negative effect of EC on AoR, CI as well as circularity factor. Hence, it was kept at the minimum level. Hence, $X_1 = 0.87$, $X_2 = 0.38$, and $X_3 = -0.89$ were selected and performed practically. It was determined by Design expert®software trial version 7.1.5.

3.7. Packability and flow parameter study of CCA of chlorzoxazone

Pure drug showed 43.6 ± 0.45 and 37.14 ± 0.2% for AoR and CI, respectively. The predicted value and experimental values obtained from regression equation and real study for Angle of repose were 21.56 and 22.14 ± 0.35, respectively (Table 9). The values for Carr's index were 15.94 and 15.08 ± 0.09, respectively. In case of CCA, encouraging results of flow properties and compressibility parameters attributed to the shape toward sphericity (Joshi, Shah, and

Table 8. Matrix of the experiments for Box–Behnken design and results for the measured responses.

Batch	dg ± S.D.[a]	CS ± S.D.[a]	S ± S.D.[a]	CI ± S.D.[a]	%Y ± S.D.[a]	DC ± S.D.[a]	CF ± S.D.[a]	HR ± S.D.[a]
01	0.351 ± 0.085	35.41 ± 0.785	0.8264 ± 0.023	14.57 ± 1.03	94.78 ± 3.62	98.54 ± 2.48	0.9912 ± 0.031	1.1707 ± 0.024
02	0.437 ± 0.112	42.44 ± 1.51	0.8095 ± 0.054	17.84 ± 2.31	95.59 ± 1.51	99.35 ± 1.98	0.9727 ± 0.052	1.2165 ± 0.032
03	0.498 ± 0.214	41.24 ± 0.965	0.9018 ± 0.022	17.09 ± 2.44	91.75 ± 2.04	95.67 ± 1.96	1.0158 ± 0.041	1.1207 ± 0.124
04	0.697 ± 2.095	47.18 ± 2.311	0.8965 ± 0.061	15.43 ± 3.23	92.47 ± 2.97	100.23 ± 1.54	1.0254 ± 0.232	1.1243 ± 0.066
05	0.566 ± 0.041	37.56 ± 0.853	0.9384 ± 0.052	14.53 ± 1.24	98.25 ± 1.91	97.84 ± 2.04	0.9041 ± 0.056	1.1701 ± 0.019
06	0.725 ± 1.310	44.25 ± 1.141	0.8571 ± 0.073	17.73 ± 2.14	99.16 ± 1.37	97.17 ± 2.35	0.9513 ± 0.037	1.1754 ± 0.046
07	0.723 ± 0.927	48.07 ± 1.367	0.9921 ± 0.071	19.33 ± 1.37	91.64 ± 2.85	98.42 ± 1.23	0.8112 ± 0.119	1.1937 ± 0.063
08	0.973 ± 0.052	54.61 ± 0.932	0.9704 ± 0.053	20.6 ± 2.78	91.07 ± 3.57	99.68 ± 1.84	0.8034 ± 0.028	1.2149 ± 0.042
09	0.479 ± 0.218	41.86 ± 0.843	0.7925 ± 0.061	14.05 ± 1.65	97.65 ± 2.11	97.75 ± 1.54	0.9221 ± 0.061	1.1703 ± 0.032
10	0.892 ± 2.046	45.55 ± 1.228	0.8765 ± 0.08	15.84 ± 2.04	98.35 ± 2.46	98.23 ± 2.31	0.9746 ± 0.241	1.1851 ± 0.084
11	0.834 ± 1.244	47.01 ± 1.637	0.8402 ± 0.033	18.56 ± 1.15	92.17 ± 1.53	101.03 ± 1.22	0.8272 ± 0.351	1.2134 ± 0.066
12	1.102 ± 2.94	49.32 ± 2.487	0.9122 ± 0.071	23.24 ± 2.81	91.83 ± 1.87	99.58 ± 2.77	0.8134 ± 0.156	1.1962 ± 0.027
13	1.009 ± 0.995	46.27 ± 3.527	0.9597 ± 0.092	14.7 ± 2.11	93.55 ± 2.34	98.24 ± 1.21	1.0548 ± 0.086	1.1781 ± 0.036
Pure drug	0.2501 ± 1.056		0.6524 ± 0.054	27.95 ± 3.21			0.6752 ± 0.217	1.21 ± 0.081

Batch	AoR ± S.D.a	a	1/b	K	k	ER ± S.D.a	TS ± S.D.a	MC ± S.D.a
01	23.81 ± 3.24	0.2581	5.1544	0.9742	0.4254	0.8158 ± 0.156	5.2155	0.7351 ± 0.112
02	22.94 ± 2.22	0.2144	9.4577	0.9534	0.3944	0.7315 ± 0.06	4.9421	0.8643 ± 0.109
03	19.07 ± 1.56	0.2396	5.181	0.9318	0.4155	0.7253 ± 0.124	5.697	1.1132 ± 0.151
04	20.18 ± 2.57	0.1509	5.3789	0.9873	0.4354	0.6971 ± 0.161	6.015	1.0108 ± 0.138
05	18.59 ± 1.28	0.1924	4.735	1.025	0.3649	0.5547 ± 0.197	4.6841	0.9965 ± 0.098
06	22.45 ± 2.08	0.2186	6.3488	0.9834	0.4966	0.7354 ± 0.165	5.248	0.9654 ± 0.147
07	27.84 ± 3.04	0.1878	9.3664	1.2142	0.5018	0.8365 ± 0.127	5.367	0.9354 ± 0.191
08	26.06 ± 2.21	0.1083	2.8547	0.9954	0.4942	0.5654 ± 0.179	6.164	0.9184 ± 0.165
09	23.51 ± 1.52	0.1612	7.6564	0.9534	0.4868	0.4682 ± 0.152	5.654	0.8157 ± 0.139
10	21.23 ± 1.63	0.1547	5.3353	0.9407	0.5057	0.5781 ± 0.104	4.9645	0.9972 ± 0.179
11	26.35 ± 2.07	0.1501	2.8069	1.106	0.4654	0.5496 ± 0.118	5.548	0.8343 ± 0.152
12	24.97 ± 3.03	0.1187	2.8476	0.9676	0.3548	0.6057 ± 0.152	5.2187	1.0173 ± 0.088
13	18.41 ± 2.14	0.095	3.7396	0.9854	0.3751	0.7653 ± 0.153	5.584	0.9735 ± 0.121
Pure drug	31.25 ± 1.56	0.1052	11.23	0.9951	0.1153	2.514 ± 0.118	1.5671	0.8512 ± 0.156

[a]Data expressed as mean ($n = 3$).

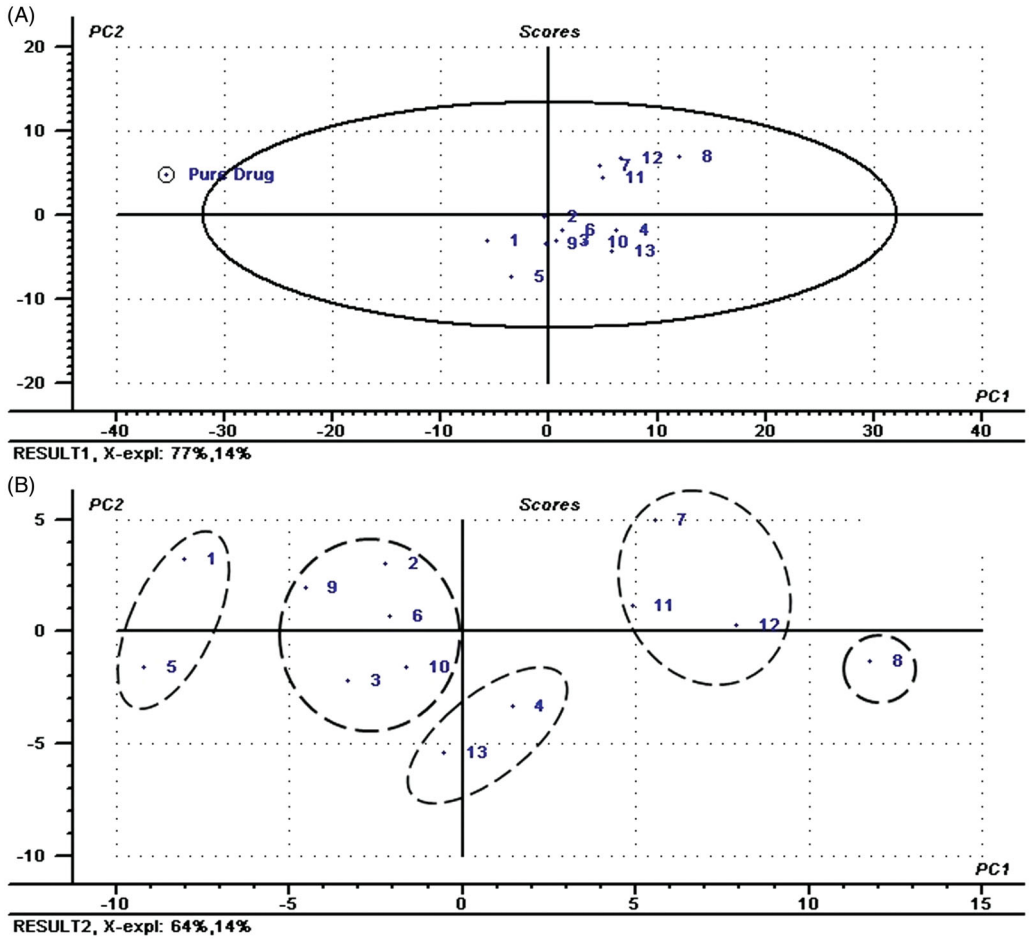

Figure 2. Score plots (A) with drug and (B) without drug for experimental design batches for Chlorzoxazone CCA.

Misra 2003). The packability parameters were ranging from 0.095 to 0.2581 for "*a*" and 2.8069 to 9.4577 for "1/*b*" (Table 8). All the batches showed remarkable improvement in its packing ability. Optimized batch showed 0.19 and 2.18 values for parameters "*a*" and "1/*b*". It was very much encouraging compared to pure drug (Patel et al. 2019).

3.8. Microscopic determination and surface topography of CCA of chlorzoxazone

As shown in Figure 6, the shape of pure drug crystals was like needle, plates, and rods with more quantity of fines resulting in more electrostatic charges which ultimately lead to very poor flow (Kumar, Chawla, and Bansal 2008).

Photomicrographs of optimized batches of CCA showed marked improvement in the surface morphology and sphericity compared to pure drug. Here, the polymers improved sphericity as well as surface smoothness. These improvements lead to improved flow due to reduced interparticulate friction (Yadav and Yadav 2009).

3.9. Drug loading efficiency and % yield of CCA

The average percentage yield of optimized batch of CCA obtained was 91 ± 2.94%. The average percentage drug content (loading) in CCA was 90.84 ± 1.24%. The results indicated good loading efficiency and %yield.

3.10. Micromeritic study

CCA of drug showed the mean diameter for all the batches in the range of 0.351 ± 0.085 to 1.102 ± 2.94 mm (Table 8). The predicted value and experimental values obtained from regression equation and real study for geometric mean diameter were 0.804 and 0.827 ± 0.091 mm, respectively (Table 9). In case of CCA, encouraging results of geometric mean diameter attributed to results as expected. The aspect ratio (AR) of optimized batch (check point batch) of CCA was 1.14. This aspect ratio of CCA near to unity was an indication of better flow property (Banga et al. 2007).

3.11. Sphericity determination of chlorzoxazone CCA

It was observed from the shape and circulatory factors that, in CCA, presence of ethyl cellulose and eudragit polymers lowered the value of shape factor and circulatory factors (Pawar et al. 2004). Overall, the shape and circularity factors were near to unity (equal to 01). This was an indication of smooth and spherical surface, which imparted good flow and compressibility. The predicted value and experimental values obtained from regression equation and real study for Circularity Factor were 0.748 and 0.805 ± 0.143, respectively (Table 9). In case of CCA, encouraging results of circularity factor attributed to sphericity of agglomerates.

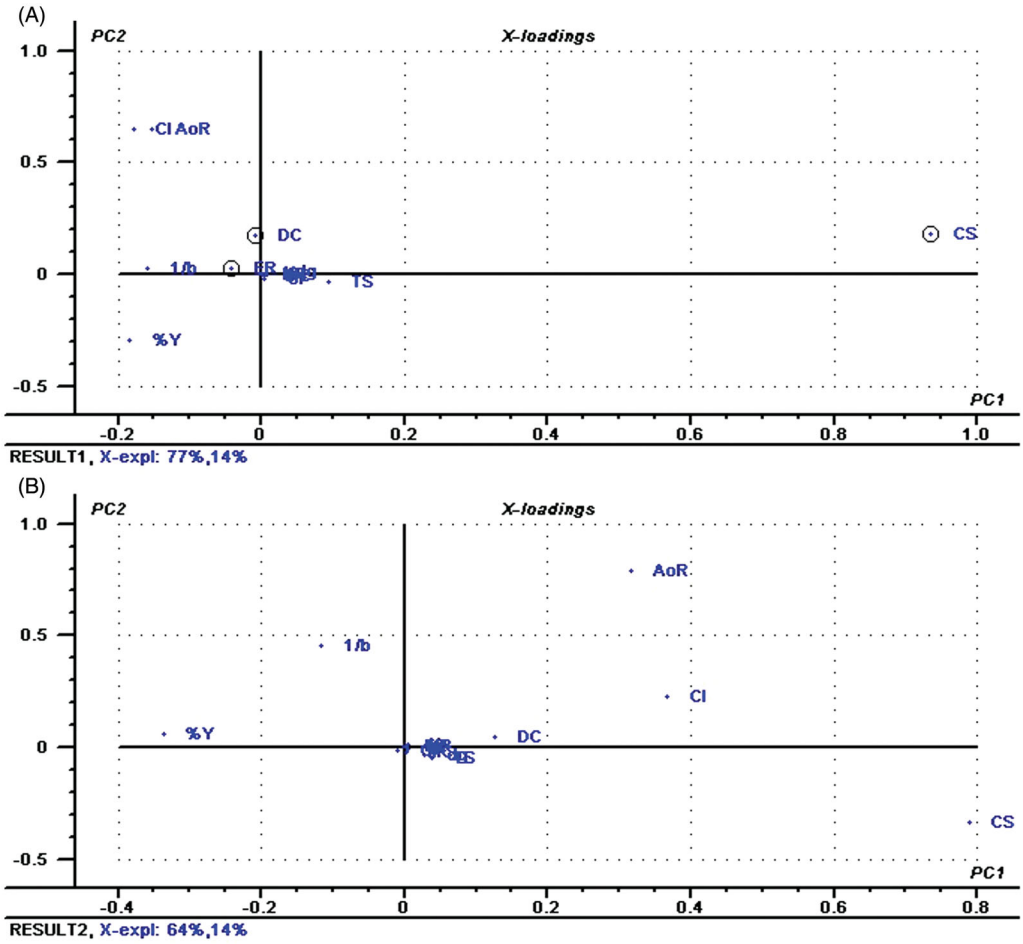

Figure 3. Loading plots (A) with drug and (B) without drug for various parameters of experimental design batches for chlorzoxazone CCA.

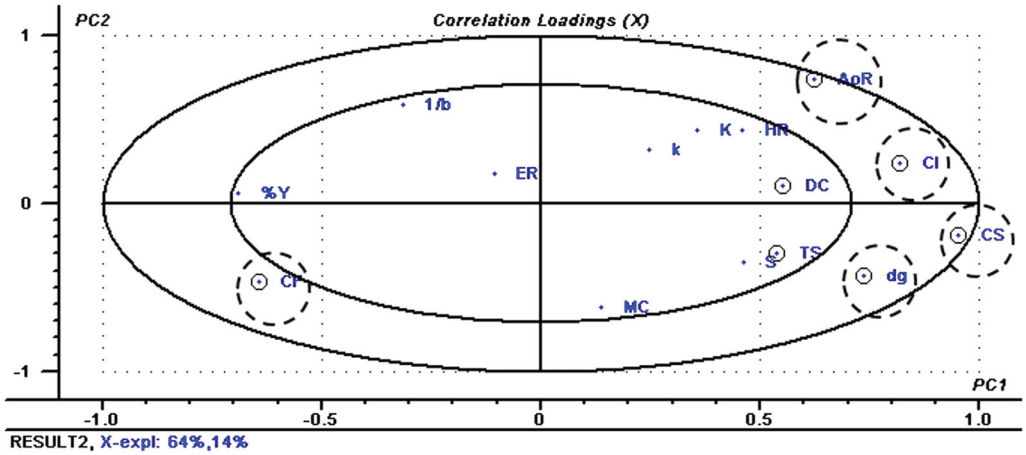

Figure 4. Correlation loading plot for screening most variable factors.

3.12. Crushing strength of CCA

The crushing strength of all the batches were ranging from 35.41 ± 0.785 g to 54.61 ± 0.932 gm (Table 8). This could be attributed to the increased agglomeration of crystals with good bridging due to presence of suitable polymers (Pawar et al. 2007). Improved crushing strength of the particles revealed the improvement in mechanical and handling properties. This was due to increased cohesive interaction between particles caused better binding and close packing between crystals (Raval et al. 2013). The crushing strength of optimized batch was 47.38 ± 0.851 g (Table 9).

3.13. Heckel plot study of optimized batch of CCA

Accurately weighed quantity of prepared samples (800 ± 5 mg) was compressed using 8 mm flat faced punch at the constant compression at different pressures ranging from 3 to 9 tons by keeping 1 min dwell time. The true

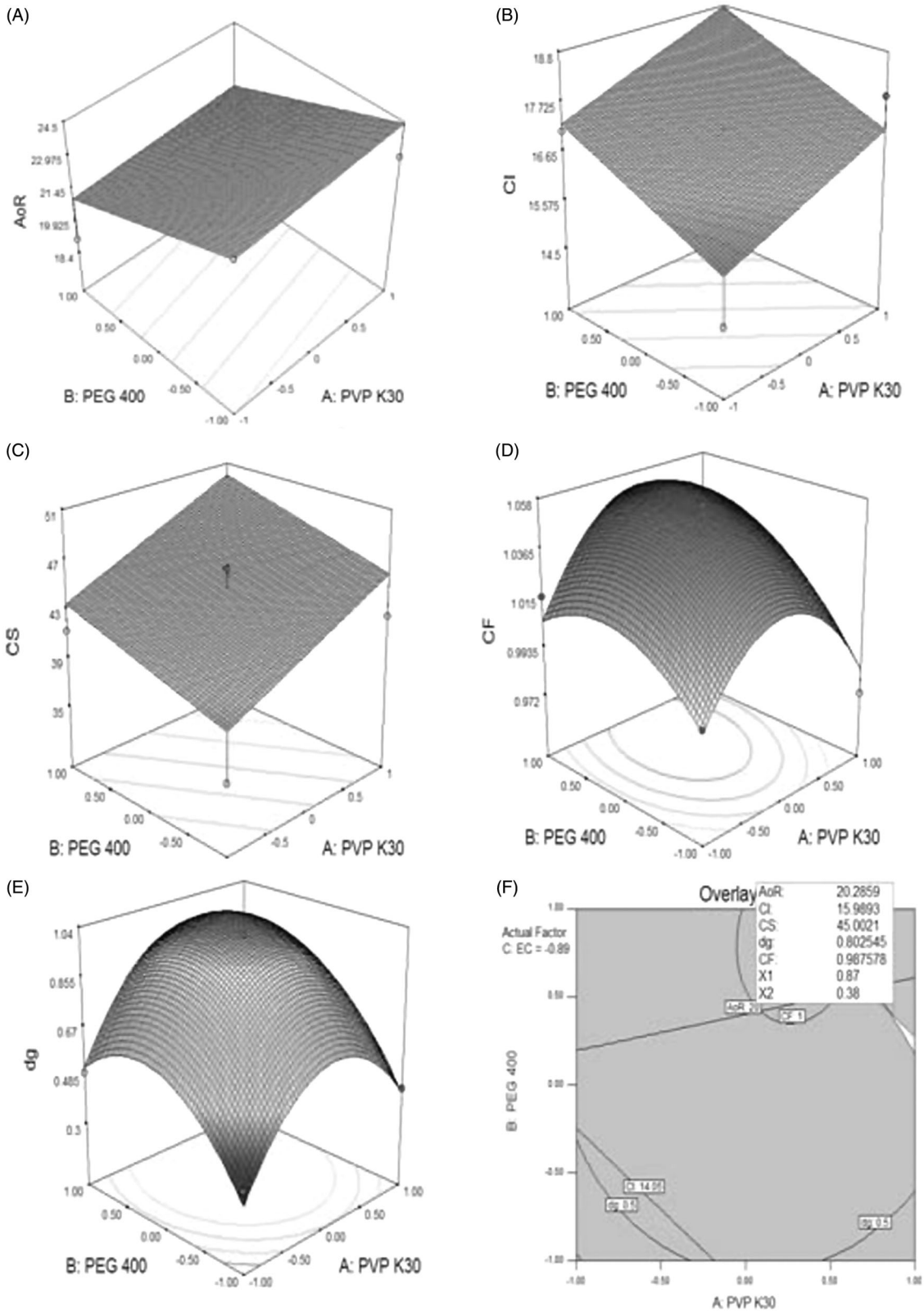

Figure 5. 3D plots for Angle of repose—AoR (A), Carr's Index—CI (B), Crushing strength—CS (C), circularity factor—CF (D), geometric mean diameter—dg (E), and overlay plot (F).

density was considered as the density of compacts when the highest pressure applied on the powder (here, 9 tons) (Maghsoodi et al. 2008; Raval et al. 2015).

The slope of Heckel plot "*K*" of optimized batch was an indicative of plastic behavior of the material (Kawashima et al. 2003). Larger the value of "*K*," greater is the plasticity in material. Table 8 shows parameters of Heckel plot of all 13 batches. "*K*" value of pure drug and optimized CCA obtained were 0.038 and 0.8132, respectively. The linearity in the graph (Figure 7) was an indication of plastic

Table 9. Results of various parameters from check point batch.

Sr. no.	Type of sample	Observations	Angle of repose ± S.D.[a]	Carr's Index ± S.D.[a] (%)	Crushing strength ± S.D.[a] (g)	Circularity Factor ± S.D.[a]	Geometric mean diameter ± S.D.[a] (mm)
1	Pure drug		43.6 ± 0.45	37.14 ± 0.2			0.2501 ± 0.106
2	From regression equation	Predicted value	21.56	15.94	46.26	0.748	0.804
3	Formulated in laboratory	Experimental value ± S.D.[a]	22.14 ± 0.35	15.08 ± 0.09	47.38 ± 0.851	0.805 ± 0.143	0.827 ± 0.091
		Percentage error	2.69	5.39	2.42	7.62	2.86

[a]Results are mean ± S.D. of three observations.

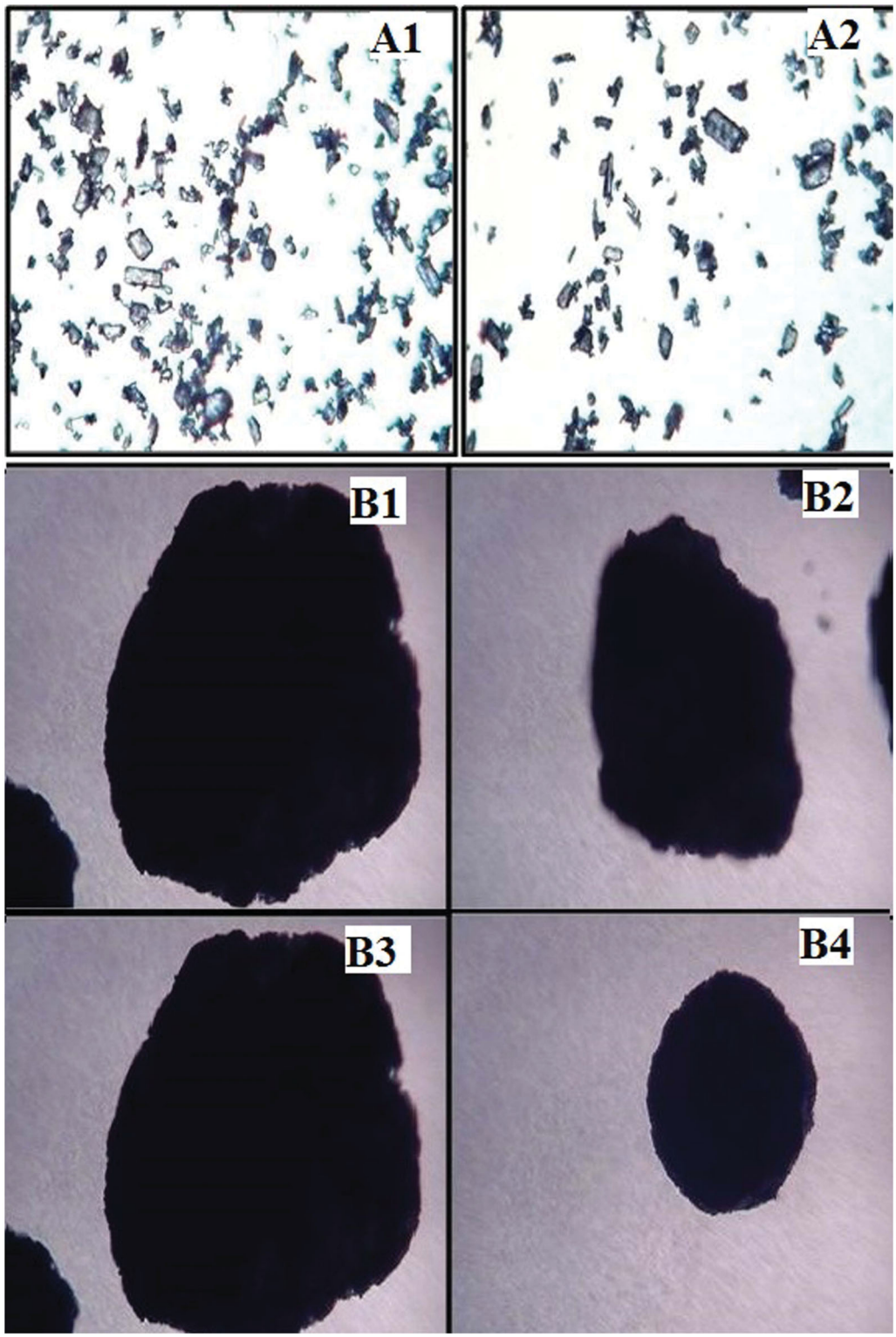

Figure 6. Microscopic photos of pure drug (A1, A2) and CCA of optimized batch (B1–B4).

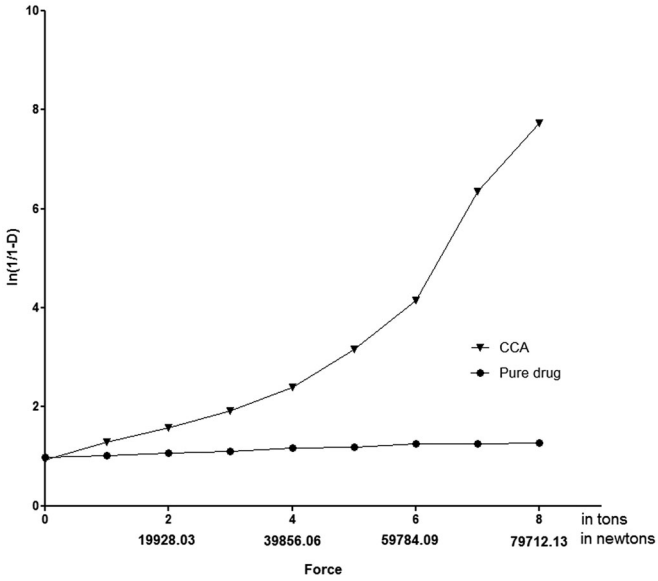

Figure 7. Heckel plot of pure drug and CCA of chlorzoxazone.

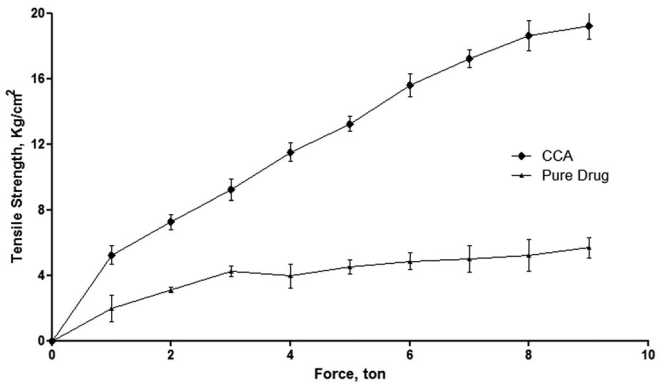

Figure 8. Pressure–tensile strength relationship for pellets of pure drug and CCA.

deformation. "*A*" value of optimized batch (0.028) was less than pure drug (0.9924). This finding suggested that low compression pressure was required to obtain closest packing of the particle, fracturing its texture, and densifying the fractured particles (Raval et al. 2015).

Yield strength (σ_0) is an indication of tendency of the materials to deform either by plastic flow or fragmentation (Paronen and Juslin 1983). Low value of yield strength (σ_0) and yield pressure (*Py*) was again an indication of low resistance to pressure, good densification, and easy compaction (Patra et al. 2007). Here, value of yield strength (σ_0) for pure drug and optimized batch of CCA was 8.7719 and 0.4099, respectively, as well as yield pressure (*Py*) values are 26.09 and 1.23, respectively. Heckel plot data suggested that all the particles were fractured easily and new surface of particles produced contributed to promote plastic deformation under applied compression pressure (Kawashima et al. 2003).

3.14. Tensile strength measurement

The maximum tensile strength was obtained at compression pressure 9 ton (pure drug – $5.708 \pm 0.621\,kg/cm^2$ and optimized CCA – $19.256 \pm 0.835\,kg/cm^2$) (Figure 8). The high tensile strength of compacts was an indication of strong inter-particulate bonding between the particles of optimized batch compared to pure drug (Patel et al. 2020).

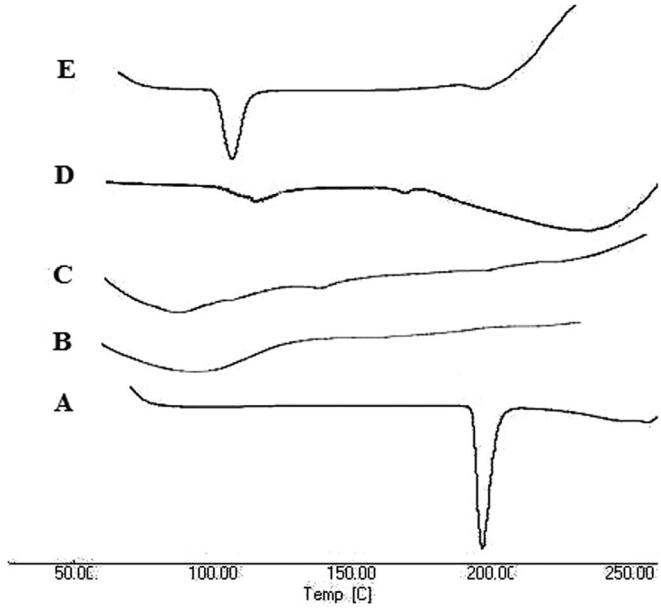

Figure 9. DSC thermograms of (A) pure drug, (B) PVP K30, (C) ethyl cellulose, (D) physical mixture of drug, PVP K-30, ethyl cellulose and PEG 400, and (E) CCA of optimized batch.

3.15. Elastic recovery of pellets after Heckel analysis

Elastic recoveries of samples were smaller than that of original drug crystals (pure drug – $5.48 \pm 0.79\%$ and optimized CCA pellets – $0.87 \pm 0.32\%$). These findings suggest that agglomerated crystals were easily fractured and the new surface of crystals produced might contribute to promote plastic deformation under compression (Raval et al. 2013).

3.16. Differential scanning calorimetry (DSC) study

In the case of DSC study, melting point of pure drug was observed at 196.13 °C (Figure 9). Melting point peak of drug was slightly broadened in thermograms of physical mixture as well as optimized agglomerates. This might be due to dispersion of crystalline drug into amorphous polymer, that is, PVP K30 and was not a sign of pharmaceutical incompatibility (Modi and Tayade 2006). Partial amorphization of drug in agglomerates might also be a reason for it. Uniformity in crystalline structure was confirmed by endothermic peaks of drug that remained at almost same temperature in physical mixture (190.40 °C) and agglomerates (201.02 °C).

3.17. Fourier transform Infrared (FT-IR) spectroscopy study

Infrared spectra of pure drug, physical mixture and prepared CCA are shown in Figure 10. The spectrum of pure drug showed the characteristic peaks at 3158.3 cm^{-1} (N–H stretch), 3052.24 cm^{-1} (aromatic hydrocarbon), 1616.3 cm^{-1}

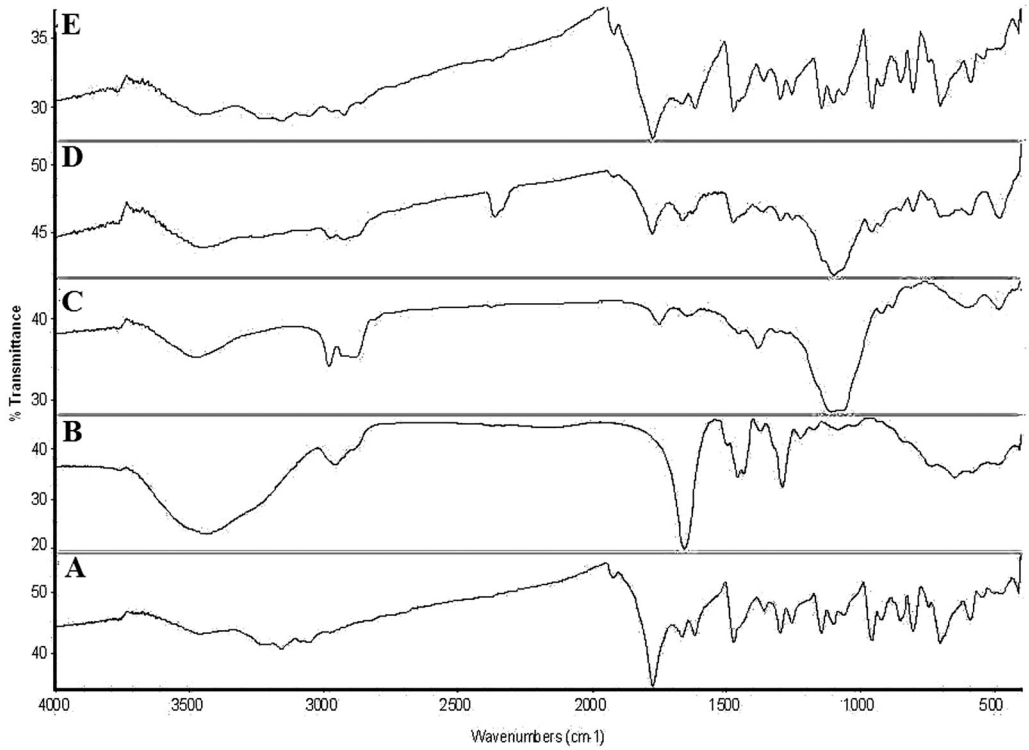

Figure 10. FT-IR spectra of (A) pure drug, (B) PVP K30, (C) ethyl cellulose, (D) physical mixture of drug, PVP K-30, ethyl cellulose and PEG 400, and (E) CCA of optimized batch.

(C = C stretch), and 732.09 cm^{-1} (C–Cl linkage). Spectra of PVP K30 showed important bands at 2959.4 cm^{-1} (C–H stretch) and stretching vibration of the carbonyl group that would typically appear around 1664.4 cm^{-1}. Moreover, a peak at about 3438.1 cm^{-1} due to O–H stretching vibrations of absorbed moisture was seen. The spectrum of ethyl cellulose showed important bands at 3478.1 cm^{-1} (–OH stretching vibrations) and the band at around 2979.2 cm^{-1} (–CH stretching vibration). All the peaks of drug were appeared in the physical mixture as well as agglomerates, which showed that there was no interaction between drug and excipients used.

3.18. Powder X-ray diffractometry (pXRD) study

Pure drug showed its characteristic peaks with decrease in percent relative intensity at 2θ values of 19.92, 27.489, 12.825, 13.815, 25.233, 17.766, and 25.796 (Figure 11). In optimized CCA of chlorzoxazone also, all XRD peaks were consistent with the pattern of pure drug crystals, indicated that there was no polymorphic changes or detection of drug-excipients incompatibility after recrystallization (Gupta et al. 2007).

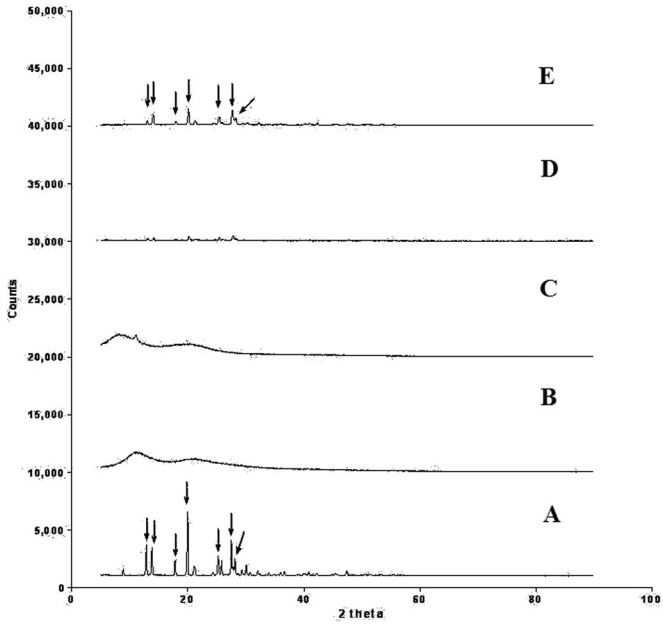

Figure 11. pXRD spectra of (A) pure drug, (B) PVP K30, (C) ethyl cellulose, (D) physical mixture of drug, PVP K-30, ethyl cellulose and PEG 400, (E) CCA of optimized batch.

3.19. Scanning electron microscopy (SEM) study

As revealed in the SEM photographs of the pure drug (Figure 12), it has very sticky and small crystals which hindered the flow (Lachman, Liberman, and Kanig 1976). The surfaces were comparatively smooth and aggregation was good when additives like PVP K30, ethyl cellulose and PEG 400 were used. Due to good agglomeration of crystals and smooth surface, the CCA prepared with addition of additives had very good sphericity, flow and compaction properties as compared to pure drug. Also, the agglomerates were very porous in nature, which increased an effective surface area and exposure of inner surfaces to dissolution fluid and ultimately improved the dissolution to a greater extent.

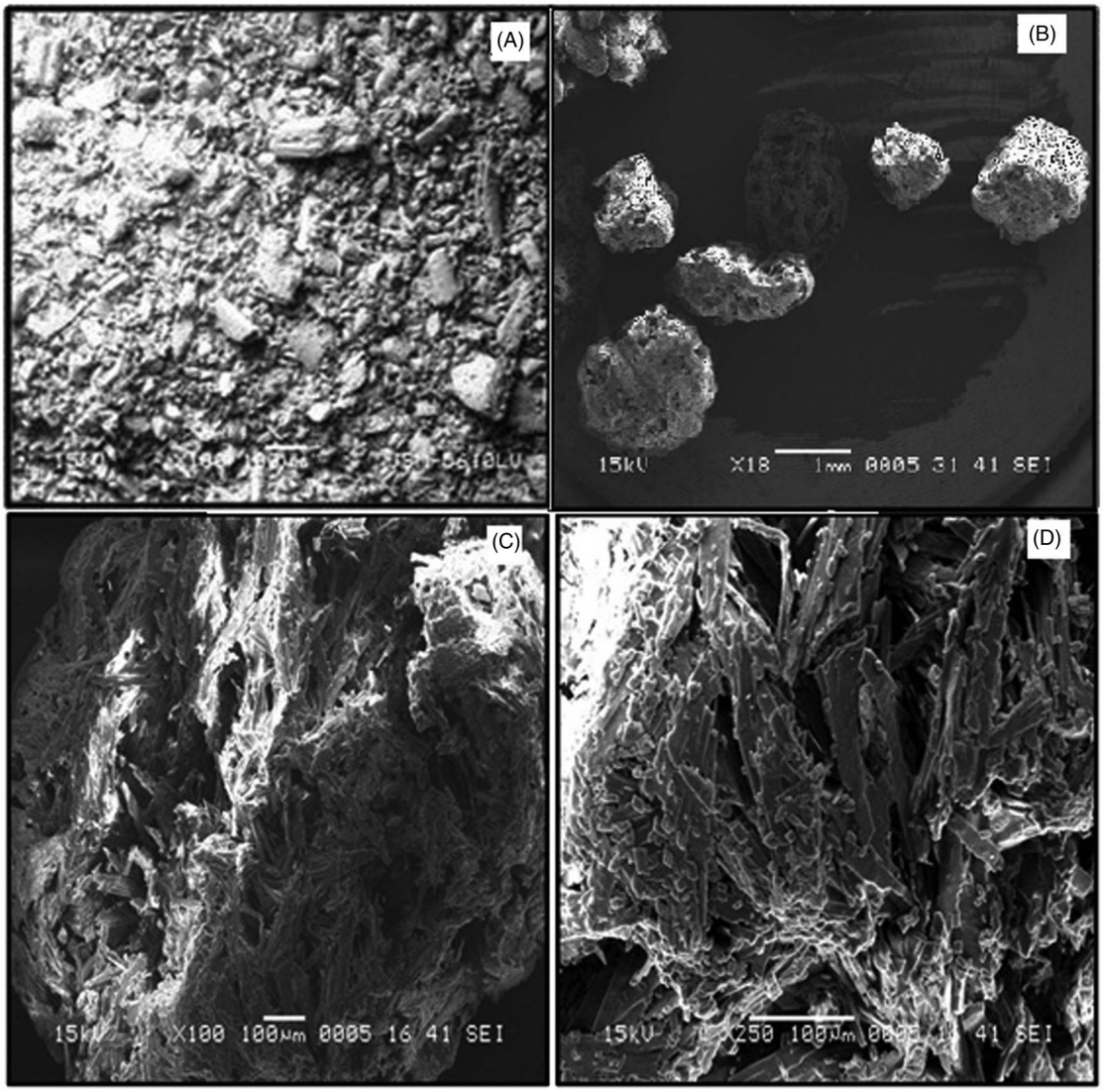

Figure 12. SEM images of (A) pure drug and (B–D) surface morphology of CCA of optimized batch.

3.20. Moisture content measurement

In all the batches, moisture content was as per the compliance with U.S. Pharmacopeia National Formulary, 1994. Maximum moisture content found was in batch no. 03 (1.1132 ± 0.151%). It was due to the presence of hygroscopic substance PEG 400 in a higher concentration (Baird et al. 2010). Overall, all the batches were containing moisture content with in the limit.

3.21. Preparation and evaluation of directly compressible tablets

Tablets containing 500 mg equivalent to Chlorzoxazone (tablet for pure drug and CCA) were prepared by direct compression using different formulation excipients as shown in Table 10. CCA were sieved to achieve similar particle size distribution (# 22) for each batch and other formulation excipients were added into it. All the ingredients for tablets prepared from CCA were weighed separately and mixed properly in "*V*" cone blender.

The material for each tablet was weighed introduced manually into the die and compressed in the tablet machine using round-shaped, 15 mm flat, concave punch.

Tablets prepared from CCA were containing very less amount of MCC (Table 10), which was a considerable improvement in the properties of drug for making directly compressible form. The formulations for tablets and its evaluations are also given in Table 10.

3.22. In vitro dissolution study

In vitro dissolution study for the prepared CCA, pure drug, and their prepared formulations was performed using USP type II apparatus. The dissolution medium was 900 ml buffer phosphate (pH 6.8) equilibrated to 37 ± 0.5 °C. Peddles/baskets were rotated at 50 RPM. The concentrations of Chlorzoxazone in the solutions were determined by UV spectrophotometer at 280 nm by diluting with phosphate buffer pH 6.8 using the same media as blank. Dissolution profile given in Figure 13 showed large improvement in the rate of drug release. Agglomerates of optimized batch

Table 10. Formulation of directly compressible tablet.

Ingredients	Pure drug	CCA
Chlorzoxazone, mg	500	532 mg (eq. to 500 mg drug)
PVP K-30, mg	16	
Ethyl cellulose, mg	16	
Kyron T-314, mg (10%)	70	65
Magnesium stearate, mg (1%)	7.0	6.5
Talc, mg (2%)	14	13
Aerosil, mg (0.5%)	3.5	3.25
MCC, mg	160	30.25
Total wt. of tablet, mg	780	650
Hardness, kg/cm^2±S.D.[a]	4.5 ± 0.31	7.6 ± 0.52
Friability, %	0.63	0.017
D.T., sec.±S.D.[a]	8.3 ± 1.23	19 ± 1.41
Diameter, mm ± S.D.[a]	12.08 ± 0.004	12.05 ± 0.006
Thickness, mm ± S.D.[a]	3.62 ± 0.055	3.37 ± 0.02
Wt. variation, mg ± S.D.[a]	777.2 ± 3.15	648.3 ± 2.56

[a]Indicates average of triplicate.

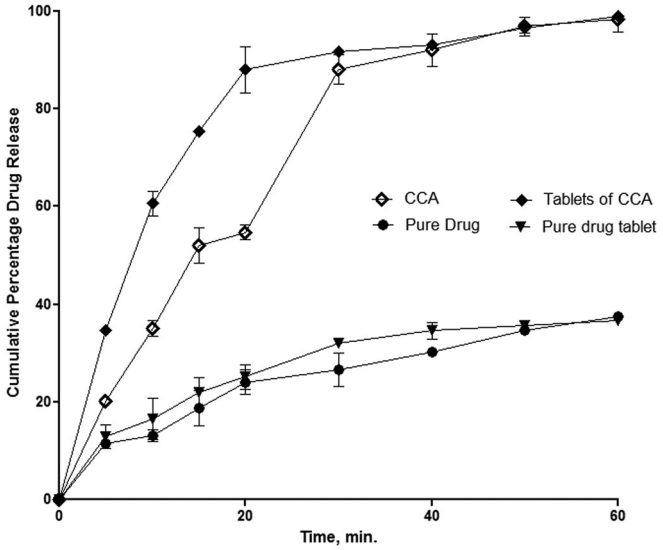

Figure 13. Dissolution profiles of chlorzoxazone pure drug, its CCA of optimized batch and their formulations.

showed 88.04 ± 2.95% (26.62 ± 3.51% for pure drug) drug release within 30 min and 98.27 ± 2.54% (37.55 ± 0.84% for pure drug) within 60 min. This might be due to hydrophilic polymer inclusion in the formulation. The greater porosity of prepared CCA (as shown in SEM photos) was also responsible for providing greater effective surface area and exposure of a large surface to the dissolution media (Vazquez et al. 2010). The solvent evaporation during formation of CCA and attrition with the stirrer might attributed toward greater porosity in the CCA.

Tablets formulated from agglomerates of optimized batch and pure drug showed 91.59 ± 0.51% (31.59 ± 0.57% for pure drug) drug release within 30 min and 98.89 ± 0.74% (36.71 ± 0.72% for pure drug) within 60 min. All the determinations were performed in triplicate.

3.23. Dissolution parameters study

The results are given in Table 11. The results shows that all the parameters were greatly improved, which was an indication of higher amorphization of drug within CCA (Dahiya 2010).

Table 11. Value of $\%DE_{10}$, $DP_{5\,min}$, and t_{50} for pure drug as well as formulation.

	$\%DE_{10}$		$DP_{5\,min}$, %		t_{50}, min	
Sample	P	T	P	T	P	T
Pure drug	8.76	9.71	11.00	13.6	–	–
CCA	18.89	32.17	20.00	30.53	14.12	7.31

P: indicates powder dissolution; T: indicates tablet dissolution.

3.24. Stability study

The amount of chlorzoxazone in the CCA was found 94.03 ± 0.21 mg after the storage. The reduction in drug content was very negligible (0.09%). The dissolution profiles of CCA before and after stability study (data not shown) was also similar. The statistical analysis also proved sameness in dissolution profile ($f_2 = 74.902$).

The dissolution profiles (data not shown) of prepared dosage forms before and after stability study of CCA were also similar. The statistical analysis of dosage form dissolution profiles of CCA before and after stability study also proved sameness ($f_2 = 84.28$).

Similar results were also observed in case of FT-IT and DSC data (not shown here) before and after stability study. From these findings, it was suggested that drug was in a stable form into the prepared CCA as well as dosage form too.

4. Conclusions

In the present work, CCA of chlorzoxazone was formulated to improve its physicochemical and mechanical properties by integrating QbD and PCA. QTPP, CQA, CPP, and CMA were identified which could affect the formation of CCA. Risk assessment was performed using Fishbone diagram. Most influencing independent factors were identified using FMEA. After applying Box–Behnken design, PCA was applied for identifying most variable dependent factors for its further controlling using response surface methodology. Prepared CCA were improved in micromeritic and mechanical properties along with its dissolution and compressibility. Reduction in crystallinity was observed in pXRD study. Scanning electron microscopy showed porous nature of CCA with spherical shape which helped in imparting better flow property and improved dissolution. Accelerated stability study indicated stable nature of drug in formulation. Overall, the study evident that use of QbD and PCA for formation of CCA in the presence of polymers/excipients as a particle engineering tool is the most helpful approach for improving the physicochemical and mechanical properties. It may be helpful to design any formulation as per the current FDA requirements. CCA has been proven as a potential approach for direct compression, instead of using a highly tiresome, lengthy, uneconomical, and complex wet granulation technology.

Acknowledgments

The authors are grateful to Evonic Degussa Incorporation Pvt. Ltd., Mumbai, India, for providing gift samples of Eudragit. Authors are thankful to Shri K. Chudasama and Shri Sheth, ERDA, Baroda, for providing the facility of SEM analysis. Authors are highly obliged to Dr. CVS Subrahmanyam—Hyderabad, Dr. A. K. Bansal, NIPER-Mohali for providing their valuable support in this study.

Disclosure statement

The authors declared no conflict of interest.

References

Anderson, N., M. Bauer, N. Boussac, R. Khan-Malek, P. Munden, and M. Sardaro. 1998. An evaluation of fit factors and dissolution efficiency for the comparison of in vitro dissolution profiles. *Journal of Pharmaceutical and Biomedical Analysis* 17 (4–5):811–22. doi: 10.1016/S0731-7085(98)00011-9.

Armstrong, N., and R. Haines-Nutt. 1974. Elastic recovery and surface area changes in compacted powder systems. *Powder Technology* 9 (5–6):287–90. doi: 10.1016/0032-5910(74)80054-9.

Asker, A. F., and C. H. Becker. 1966. Some spray-dried formulations of Sulfaethylthiadiazole for prolonged-release medication. *Journal of Pharmaceutical Sciences* 55 (1):90–4. doi: 10.1002/jps.2600550119.

Aulton, M. 2007. *Pharmaceutics: The design and manufacture of medicines*. 3rd ed. London, UK: Elsevier.

Autamashih, M., A. Isah, T. Allagh, and M. Ibrahim. 2011. Heckel and Kawakita analyses of granules of the crude leaves extract of vernonia galamensis prepared using gelatin as binder. *International Journal of Pharmaceutical Sciences and Research* 2:2566–71.

Baird, J., R. Olayo-Valles, C. Rinaldi, and L. Taylor. 2010. Effect of molecular weight, temperature, and additives on the moisture sorption properties of polyethylene glycol. *Journal of Pharmaceutical Sciences* 99 (1):154–68. doi: 10.1002/jps.21808.

Banga, S., G. Chawla, D. Varandani, B. Mehta, and A. Bansal. 2007. Modification of the crystal habit of celecoxib for improved processibility. *Journal of Pharmacy and Pharmacology* 59 (1):29–39. doi: 10.1211/jpp.59.1.0005.

Bhattacharyya, S., I. Bhattacharyya, and N. Patro. 2010. Standardization and optimization of micromeritic properties of nimesulide for processing into a tablet dosage form by crystallo-co-agglomeration technology. *Asian Journal of Pharmaceutics* 4 (1):24–7. doi: 10.4103/0973-8398.63980.

Bose, P., S. Damineni, M. Varma, and S. Dathrika. 2011. Influence of various bridging liquids on spherical agglomerates of Indomethacin. *International Journal of Research in Pharmaceutical Sciences* 2: 147–57.

Chandresh, P., N. Malay, and B. Prajapati. 2018. "Crystallo Co Agglomeration" the novel approach for microparticulation. *Research and Review on Health Care: Open Access Journal* 1:01–7.

Chatterjee, A., M. Gupta, and B. Srivastava. 2017. Spherical crystallization: A technique use to reform solubility and flow property of active pharmaceutical ingredients. *International Journal of Pharmaceutical Investigation* 7 (1):4–9. doi: 10.4103/jphi.JPHI_36_16.

Chaulang, G., K. Patil, D. Ghodke, and S. Khan. 2008. Preparation and characterization of solid dispersion tablet of furosemide with crospovidone. *Research J Pharmaceutical Technology* 1:386–9.

Chavda, V., and R. Maheshwari. 2008. Tailoring of ketoprofen particle morphology via novel crystallo-co-agglomeration technique to obtain a directly compressible material. *Asian Journal of Pharmaceutics* 2 (1):61–7. doi: 10.4103/0973-8398.41569.

Chopra, S., S. Motwani, Z. Iqbal, S. Talegaonkar, F. Ahmad, and R. Khar. 2007. Optimisation of polyherbal gels for vaginal drug delivery by Box-Behnken statistical design. *European Journal of Pharmaceutics and Biopharmaceutics* 67 (1):120–31. doi: 10.1016/j.ejpb.2006.12.013.

Chouracia, M., V. Jain, S. Jain, and N. Jain. 2004. Preparation and characterization of spherical crystal agglomerates for direct tabletting by the spherical crystallization technique. *Indian Drugs* 41:214–20.

Dahiya, S. 2010. Studies on formulation development of a poorly water-soluble drug through solid dispersion technique. *Thai Journal of Pharmaceutical Sciences* 34:77–87.

Deshkar, S., R. Borde, R. Kale, B. Waghmare, and A. Thomas. 2017. Formulation of cilostazol spherical agglomerates by crystallo-co-agglomeration technique and optimization using design of experimentation. *International Journal of Pharmaceutical Investigation* 7 (4):164–73. doi: 10.4103/jphi.JPHI_39_17.

Deshpande, M., K. Mahadik, A. Pawar, and A. Paradkar. 1997. Evaluation of spherical crystallization as particle size enlargement technique for Aspirin. *Indian Journal Pharmaceutical Sciences* 59: 32–4.

Fahmy, R., R. Kona, R. Dandu, W. Xie, G. Claycamp, and S. Hoag. 2012. Quality by design I: Application of failure mode effect analysis (FMEA) and Plackett-Burman design of experiments in the identification of "main factors" in the formulation and process design space for roller-compacted ciprofloxacin hydrochloride immediate-release tablets. *AAPS PharmSciTech* 13 (4):1243–54. doi: 10.1208/s12249-012-9844-x.

Fernádez-Arévalo, M., M. T. Vela, and A. M. Rabasco. 1990. Rheological study of lactose coated with acrylic resins. *Drug Development and Industrial Pharmacy* 16 (2):295–300. doi: 10.3109/03639049009114887.

Florey, C. 1987. *Analytical profiles of drug substances*, Vol. 16. London, UK: Academic press Inc.

Garala, K., J. Patel, A. Dhingani, and A. Dharamsi. 2013. Preparation and evaluation of agglomerated crystals by crystallo-co-agglomeration: An integrated approach of principal component analysis and Box-Behnken experimental design. *International Journal of Pharmaceutics* 452 (1–2):135–56. doi: 10.1016/j.ijpharm.2013.04.073.

Garg, R., and G. Gupta. 2010. Gastro retentive floating microspheres of Silymarin: Preparation and in vitro evaluation. *Tropical Journal of Pharmaceutical Research* 9 (1):59–66. doi: 10.4314/tjpr.v9i1.52037.

Grau, M., O. Kayser, and R. Muller. 2000. Nanosuspension of poorly soluble drugs – Reproducibility of small scale production. *International Journal of Pharmaceutics* 196 (2):155–7. doi: 10.1016/S0378-5173(99)00411-1.

Gupta, V., S. Mutalik, M. Patel, and G. Jani. 2007. Spherical crystals of celecoxib to improve solubility, dissolution rate and micromeritic properties. *Acta Pharmaceutica* 57 (2):173–84. doi: 10.2478/v10007-007-0014-8.

Hancock, B. C., and G. Zografi. 1997. Characteristics and significance of the amorphous state in pharmaceutical systems. *Journal of Pharmaceutical Sciences* 86 (1):1–12. doi: 10.1021/js9601896.

Haware, R., I. Tho, and A. Bauer-Brandl. 2009. Application of multivariate methods to compression behavior evaluation of directly compressible materials. *European Journal of Pharmaceutics and Biopharmaceutics: Official Journal of Arbeitsgemeinschaft Fur Pharmazeutische Verfahrenstechnik e.V* 72 (1):148–55. doi: 10.1016/j.ejpb.2008.11.008.

Hector, N., B. Anailien, G. Rolando, M. Dulce, and V. Marilo. 2000. Physico-chemical and solid-state characterization of secnidazole. *Il Farmaco* 55:700–7.

Heng, P., T. Wong, and L. Chan. 2000. Influence of production variables on the sphericity of melt pellets. *Chemical & Pharmaceutical Bulletin* 48 (3):420–4. doi: 10.1248/cpb.48.420.

Jadhav, N., A. Pawar, and A. Paradkar. 2007. Design and evaluation of deformable talc agglomerates prepared by crystallo-co-agglomeration technique for generating heterogeneous matrix. *AAPS PharmSciTech* 8 (3):E61–E67. doi: 10.1208/pt0803059.

Jadhav, N., A. Pawar, and A. Paradkar. 2010. Effect of drug content and agglomerate size on tabletability and drug release characteristics of Bromhexine hydrochloridetalc agglomerates prepared by crystallo-co-agglomeration. *Acta Pharmaceutica (Zagreb, Croatia)* 60 (1): 25–38. doi: 10.2478/v10007-010-0002-2.

Jakob, K. 2006. Investigation of a 2-step agglomeration process performed in a rotary processor using polyethylene glycol solutions as the primary binder liquid. *AAPS PharmSciTech* 7:E1–E8.

Jayasankar, A., A. Somwangthanaroj, Z. J. Shao, and N. Rodríguez-Hornedo. 2006. Cocrystal formation during cogrinding and storage is mediated by amorphous phase. *Pharmaceutical Research* 23 (10): 2381–92. doi: 10.1007/s11095-006-9110-6.

Joshi, A., S. Shah, and A. Misra. 2003. Preparation and evaluation of directly compressible forms of rifampicin and ibuprofen. *Indian Journal of Pharmaceutical Sciences* 65:232–8.

Kadam, S., K. Mahadik, and A. Paradkar. February 1997a. Vidyapeeth B, assignee. A process for making agglomerates for use as or in a drug delivery system. *Indian Patent* 183036.

Kadam, S., K. Mahadik, and A. Paradkar. February 1997b. Vidyapeeth B, assignee. A process for making agglomerates for use as or in a drug delivery system. *Indian Patent* 183481.

Kawashima, Y., M. Imai, H. Takeuchi, H. Yamamoto, K. Kamiya, and T. Hino. 2003. Improved flowability and compactibility of spherically agglomerated crystals of ascorbic acid for direct tableting designed by spherical crystallization process. *Powder Technology* 130 (1–3):283–9. doi: 10.1016/S0032-5910(02)00206-1.

Kawashima, Y., M. Okumura, and H. Takenaka. 1982. Spherical crystallization: Direct spherical agglomeration of Salicylic acid crystals during crystallization. *Science* 216 (4550):1127–8. doi: 10.1126/science.216.4550.1127.

Kawashima, Y., M. Okumura, H. Takenaka, and A. Kojima. 1984. Direct preparation of spherically agglomerated salicylic acid crystals using crystallization. *Journal of Pharmaceutical Sciences* 73 (11): 1535–8. doi: 10.1002/jps.2600731110.

Kumar, S., G. Chawla, and A. Bansal. 2008. Role of additives like polymers and surfactants in the crystallization of mebendazole. *Yakugaku Zasshi : Journal of the Pharmaceutical Society of Japan* 128 (2):281–9. doi: 10.1248/yakushi.128.281.

Lachman, L., H. Liberman, and J. Kanig. 1976. *Theory and practice of industrial pharmacy*. 2nd ed. Philadelphia, PA: Lea & Febiger.

Lachman, L., H. Libermann, and J. Kanig. 1991. *The theory and practice of industrial pharmacy*. 3rd ed. Bombay, India: Varghese Publishers.

Maghsoodi, M., O. Taghizadeh, G. Martin, and A. Nokhodchi. 2008. Particle design of naproxen-disintegrant agglomerates for direct compression by a crystallo-co-agglomeration technique. *International Journal of Pharmaceutics* 351 (1–2):45–54. doi: 10.1016/j.ijpharm.2007.09.033.

Manoj, K., P. Seenivasan, K. Arul, and M. Senthil Kumar. 2019. Study of the effect of pvp k30 in the enhancement of solubility of telmisartan by polymer assisted crystal agglomeration using polymer enriched bridging liquid technique. *International Journal of Research in Pharmaceutical Sciences* 10:2290–9.

Martin, A., J. Swarbrick, and A. Cammarata. 1991. *Physical pharmacy: Physical chemical principles in the pharmaceutical sciences*. 3rd ed. Bombay, India: Varghese Publishers.

Maurya, D., Y. Sultana, M. Aqil, D. Kumar, K. Chuttani, A. Ali, and A. Mishra. 2011. Formulation and optimization of alkaline extracted ispaghula husk microparticles of isoniazid – in vitro and in vivo assessment. *Journal of Microencapsulation* 28 (6):472–82. doi: 10.3109/02652048.2011.580861.

Modi, A., and P. Tayade. 2006. Enhancement of dissolution profile by solid dispersion (kneading) technique. *AAPS PharmSciTech* 7 (3): E1–E6. doi: 10.1208/pt070368.

Paradkar, A., A. Pawar, and N. Jadhav. 2010. Crystallo-co-agglomeration: A novel particle engineering technique. *Asian Journal of Pharmaceutics* 4 (1):4–10. doi: 10.4103/0973-8398.63975.

Paradkar, A., K. Mahadik, and A. Pawar. 1998. Spherical crystallization a novel particle design technique. *Indian Drugs* 31:283–99.

Paradkar, A., M. Maheshwari, A. R. Ketkar, and B. Chauhan. 2003. Preparation and evaluation of Ibuprofen beads by melt solidification technique. *International Journal of Pharmaceutics* 255 (1–2):33–42. doi: 10.1016/S0378-5173(03)00081-4.

Paradkar, A., M. Maheshwari, and H. Jahagirdar. 2005. Melt sonocrystallisation of Ibuprofen: Effect on crystal properties. *European Journal of Pharmaceutical Sciences* 25:41–8.

Paronen, P., and M. Juslin. 1983. Compressional characteristics of four starches. *The Journal of Pharmacy and Pharmacology* 35 (10): 627–35. doi: 10.1111/j.2042-7158.1983.tb02855.x.

Patel, R., M. Raval, A. Bagathariya, and N. Sheth. 2019. Functionality improvement of Nimesulide by eutectic formation with nicotinamide: Exploration using temperature-composition phase diagram. *Advanced Powder Technology* 30 (5):961–73. doi: 10.1016/j.apt.2019.02.010.

Patel, R., M. Raval, and N. Sheth. 2020. Formation of Diacerein–fumaric acid eutectic as a multi-component system for the functionality enhancement. *Journal of Drug Delivery Science and Technology* 58:101562. doi: 10.1016/j.jddst.2020.101562.

Patra, N., S. Singh, P. Hamd, and M. Vimladevi. 2007. A sysyematic study on micromeritic properties and consolidation behavior of the terminaliya arjuna bark powder for processing into tablet dosage form. *International Journal of Pharmaceutical Excipients* 6:6–7.

Pawar, A., A. Paradkar, S. Kadam, and K. Mahadik. 2004. Crystallo-co-agglomeration: A novel process to obtain ibuprofen-paracetamol agglomerates. *AAPS PharmSciTech* 5 (3):57–64. doi: 10.1208/pt050344.

Pawar, A., A. Paradkar, S. Kadam, and K. Mahadik. 2007. Effect of polymers on crystallo-co-agglomeration of ibuprofen–paracetamol: Factorial design. *Indian Journal of Pharmaceutical Sciences* 69 (5): 658–64. doi: 10.4103/0250-474X.38471.

Piera, D., S. Mara, and J. Etienne. 2001. The spray drying of acetazolamide as a method to modify crystal properties and to improve compression behavior. *International Journal of Pharmaceutics* 213: 209–21.

Raval, M., K. Sorathiya, N. Chauhan, J. Patel, R. Parikh, and N. Sheth. 2013. Influence of polymers/excipients on development of agglomerated crystals of Secnidazole by crystallo-co-agglomeration technique to improve processability. *Drug Development and Industrial Pharmacy* 39 (3):437–46. doi: 10.3109/03639045.2012.662508.

Raval, M., P. Vaghela, A. Vachhani, and N. Sheth. 2015. Role of excipients in the crystallization of Albendazole. *Advanced Powder Technology* 26 (4):1102–15. doi: 10.1016/j.apt.2015.05.006.

Ribardière, A., P. Tchoreloff, G. Couarraze, and F. Puisieux. 1996. Modification of ketoprofen bead structure produced by the spherical crystallization technique with a two-solvent system. *International Journal of Pharmaceutics* 144 (2):195–207. doi: 10.1016/S0378-5173(96)04746-1.

Ring, T. 1991. Kinetic effects on particle morphology and size distribution during batch precipitation. *Powder Technology* 65 (1–3): 195–206. doi: 10.1016/0032-5910(91)80182-I.

Sarwar, B., P. Sandhu, R. Batra, R. Khurana, and B. Singh. 2015. QbD-based systematic development of novel optimized solid self-nanoemulsifying drug delivery systems (SNEDDS) of lovastatin with enhanced biopharmaceutical performance. *Drug Delivery* 22 (6): 765–84. doi: 10.3109/10717544.2014.900154.

Sekikawa, H., M. Nakano, and T. Arita. 1978. Inhibitory effect of polyvinyl pyrollidone on the crystallization of drugs. *Chemical & Pharmaceutical Bulletin* 26 (1):118–26. doi: 10.1248/cpb.26.118.

Thapa, P., D. H. Choi, M. S. Kim, and S. H. Jeong. 2019. Effects of granulation process variables on the physical properties of dosage forms by combination of experimental design and principal component analysis. *Asian Journal of Pharmaceutical Sciences* 14 (3): 287–304. doi: 10.1016/j.ajps.2018.08.006.

Vazquez, D., S. Takagi, S. Frukhtbeyn, and L. Chow. 2010. Effects of addition of mannitol crystallization the porosity and dissolution rate of a calcium phosphate cement. *Journal of Research of the National Institute of Standards and Technology* 115 (4):225–32. doi: 10.6028/jres.115.016.

Vogt, M., K. Kunath, and J. Dressman. 2008. Dissolution enhancement of Fenofibrate by micronization, cogrinding and spray-drying: Comparison with commercial preparations. *European Journal of Pharmaceutics and Biopharmaceutics* 68 (2):283–8. doi: 10.1016/j.ejpb.2007.05.010.

Vora, C., R. Patadia, K. Mittal, and R. Mashru. 2013. Risk based approach for design and optimization of stomach specific delivery of rifampicin. *International Journal of Pharmaceutics* 455 (1–2):169–81. doi: 10.1016/j.ijpharm.2013.07.043.

Woodruff, C., and N. Nuessle. 1972. Effect of processing variables on particles obtained by extrusion-spheronization processing. *Journal of Pharmaceutical Sciences* 61 (5):787–90. doi: 10.1002/jps.2600610525.

Yadav, V., and A. Yadav. 2009. Polymeric recrystallized agglomerates of cefuroxime axetil prepared by emulsion solvent diffusion technique. *Tropical Journal of Pharmaceutical Research* 8 (4):361–9. doi: 10.4314/tjpr.v8i4.45225.

Yehia, K. 2007. Roll press prototype design for fine powders agglomeration. *Journal of Applied Sciences Research* 3:1275–8.

Zaborenko, N., Z. Shi, C. C. Corredor, B. M. Smith-Goettler, L. Zhang, A. Hermans, C. M. Neu, M. A. Alam, M. J. Cohen, X. Lu, et al. 2019. First-principles and empirical approaches to predicting in vitro dissolution for pharmaceutical formulation and process development and for product release testing. *The AAPS Journal* 21 (3):1–20. doi: 10.1208/s12248-019-0297-y.

Zhang, L., G. Chai, X. Zeng, H. He, H. Xu, and X. Tang. 2010. Preparation of fenofibrate immediate-release tablets involving wet grinding for improved bioavailability. *Drug Development and Industrial Pharmacy* 36 (9):1054–63. doi: 10.3109/03639041003642081.